The Pennsylvania State University

The Graduate School

College of Engineering

EFFICIENT DETECTION OF UV LIGHT BY QUANTUM DOTS SENSITIZED SILICON DETECTOR

A Thesis in

Electrical Engineering

by

YASH THAKUR

Submitted in Partial Fulfillment
of the Requirements
for the Degree of

Master of Science

August 2014

The thesis of Yash Thakur was reviewed and approved* by the following:

Jerzy Ruzyllo
Distinguished Professor of Electrical Engineering
Thesis Advisor

Noel (Chris) Geibink
Assistant Professor of Electrical Engineering

Kultegin Aydin
Professor of Electrical Engineering
Head of the Department

*Signatures are on file in the Graduate School

ABSTRACT

Historically, light coming from the sun has been our prime source of light energy. It is crucial for various applications to detect and utilize the invisible part beyond violet. The detection of ultraviolet (UV) radiation has been of great interest for industrial, medical, military, and environmental applications. Therefore, it is important to make simple, accurate, reliable, and low cost instruments to detect UV. Silicon detectors are the most common and inexpensive commercial solutions available for UV detection. However, they show poor performance in ultraviolet region. In this thesis, the red CdSe/ZnS core-shell quantum dots are used to improve the response of the silicon detector by downshifting the UV light to peak sensitive wavelength of silicon.

In this study, an improvement in average external quantum efficiency of 51% in the near UV (300-400 nm) region has been confirmed using a 40 nm thick layer of CdSe/ZnS quantum dots. The short circuit current is improved by a factor of 6 under laser excitation of 405 nm. CdSe/ZnS core-shell quantum dots were chosen for this study because of their direct band gap and size tunable wavelength properties, which span over the entire visible spectrum. The size selection of the quantum dots was based on emission wavelength. The ultra-thin layer of quantum dots has been deposited using the mist deposition tool. The results demonstrate that the quantum dots can be used as an alternative to phosphors for down-shifting the ultra violet light in silicon UV detectors.

TABLE OF CONTENTS

LIST OF FIGURES

LIST OF TABLES

ACKNOWLEDGEMENTS

I would like to express my sincere gratitude to Dr. Jerzy Ruzyllo for his constant support and guidance throughout this endeavor. Under his tutelage, I have grown as an individual, both academically and personally. He has instilled optimism and patience in me, which have been crucial for completion of my graduate studies. I am deeply grateful to Dr. Chris Geibink for being the Co-Chair of my committee, and his valuable inputs. I am thankful to him for letting me use his lab for the experiments. I am thankful to Jared Price for helping me out with the equipment in his lab, building custom equipment and his constant support as a friend.

I would like to thank Ju-Hung for training me on the mist deposition tool. I am grateful to Aditya Kshirsagar for educating me about the tool, and the valuable discussions on phone. I am highly indebted to Dr. S Ashok for helping me understand the physics of detectors. I am grateful to him for his sound advice and financial assistance in times of need.

I want to thank my beloved parents- Namita and Balwant Singh, and my grandmother Indra Shukla for their constant support and encouragement. I am grateful to my Aunt Amita Dave, Uncle Atul Dave, and Uncle Vasu Misra for their constant guidance. I would like to dedicate my thesis to my late Grandfather K.B. Shukla.

Chapter 1

Introduction

Ultraviolet (UV) is an electromagnetic radiation that ranges from 10 nm to 400 nm. In 1801, a German physicist, Johann Wilhelm Ritter, discovered the existence of ultraviolet light. In a simple experiment, he showed that the invisible rays, which were beyond the violet end of the spectrum, darkened silver chloride more efficiently than visible light. It was thus coined as "ultraviolet" because the spectrum consisted of electromagnetic waves with frequencies higher than those which humans identify as the violet color [1]. Ultraviolet region is subdivided into UVA (400-320 nm), UVB (320-280 nm), and UVC (280-10 nm) [2]. The table 1-1 shows the other classifications, which are widely used in the literature.

The ultraviolet research began to receive attention in the latter half of the 19^{th} century. The stratospheric ozone limited the wavelengths reaching the surface of the Earth to about 300 nm. This set the limitations on terrestrial ultraviolet research. The molecular oxygen absorbs ultraviolet below 200 nm; this limits the laboratory spectrograph, unless it is placed in a vacuum chamber. Thus, the wavelengths shorter than 200 nm are also called vacuum ultraviolet. At that time, the lack of good vacuum, and other associated technology was a hindrance to further research. Secondly, the poor transmission and reflection of materials failed the optical methods used in the visible spectrum [3].

Table 1-1. Other classifications of UV [1].

Sub-range	Wavelength Range (nm)
Near-UV (NUV)	400-300
Middle-UV (MUV)	300-200
Far-UV (FUV)	200-100
Deep-UV (DUV)	350-190
Vacuum-UV (VUV)	200-10
Extreme-UV (EUV)	100-10

The exploration of space in 1940's opened up new doors for ultra violet research. It provided the impetus for better instrumentation, which included better windows, gratings, filters, detectors, and light sources. It also pressed for improvement in spectroscopy of the atoms, molecules, and ions of planetary and stellar atmospheres, and reliable standards for calibrations [3].

Most commercial p-n junction photo detectors are designed to detect a specific band of electromagnetic spectrum efficiently [4]. The challenging part of the ultraviolet spectral range for silicon based photo detector is between 100-400 nm. The penetration depth of these high energy photons is extremely shallow. Therefore, the ultraviolet light is primarily absorbed near the surface. The recombination near the surface is very high due to the presence of surface states. Thus, leading to a poor response in the ultraviolet region.

There are two primary ways to improve the response of silicon photovoltaic detectors in ultraviolet region. First, use of advanced design concepts, and manufacturing processes to make ultra-shallow junctions, use of low doping levels, or very thin window/buffer layers. However, these steps can be difficult as well as expensive to implement, and may decrease device efficiency [5]. The second method is to down-shift the incident light using luminescent downshifting materials.

The quantum dots offer useful advantages as luminescent downshifting materials. They exhibit a wide absorption band, high emission intensity, and relatively good photo stability. Since the quantum dots are inorganic crystals, chemical bond changes require additional energy for atomic displacement into an interstitial lattice location [6]. Therefore, the quantum dots are expected to resist photo bleaching, and radiation damage. The work done by Cress C. et al. showed that quantum dots are more resistive to radiation damage

than bulk [7]. The quantum dots are very large in comparison to a dye molecule so they resist pinhole formation.

This study demonstrates the luminescent down-shifting principle by using the CdSe/ZnS quantum dots. The experimental results show improvement in the response of the silicon photodiode in ultraviolet region. Mist deposition tool has been used to deposit ultra-thin films of these quantum dots.

Chapter 2 gives the background of ultraviolet detectors, introduces luminescent down-shifting materials, physics of quantum dots, and details of mist deposition tool. Chapter 3 covers the scope, and motivation behind the project. Chapter 4 explains the experimental procedure used in this study. Chapter 5 sums up the results and discussion part. In the end, the complete project is summarized in Chapter 6.

Chapter 2

Background

This chapter introduces the needs and challenges of ultraviolet detection. It describes the state of the art UV detectors. It introduces the luminescent down-shifting materials, and follows with the detailed explanation of quantum dots. It explains about mist deposition tool, sources of UV, and its applications.

2.1 UV Detection: Needs and Challenges

The observation and recording of the ultraviolet from astronomical objects such as planets in our solar system, stars, nebulae and galaxies enable us to gain extra information, such as temperature, and chemical composition of these objects [8]. However, most of the ultraviolet is absorbed by the ozone layer. Therefore, these observations need to be made outside the Earth's Stratosphere. In the space station, the Hubble Space Telescope, the Faint Object Spectrograph (FOS), and the Goddard High Resolution Spectrograph (GHRS) are used to collect, and analyze the ultraviolet coming from these distant objects. The Solar and Heliospheric Observatory (SOHO) is a spacecraft that was launched in 1995 to study the Sun [8]. Two of SOHO's twelve instruments are used to record, and analyze ultraviolet radiation from the Sun.

The vitamin D enriched sunlight is essential for human body. When our skin is exposed to UV B, it stimulates the production of vitamin D. But, too much exposure to UV

B can cause skin cancer. Hence, ultraviolet detectors are used in UV dosimeters to monitor the amount of UV absorbed. Ultraviolet detectors can detect ultraviolet emissions from flames in the presence of hot backgrounds (such as infrared emission from the hot bricks in a furnace). This provides an excellent flame on/off determination system for controlling the gas supply to large furnaces and boiler systems. Earth's atmosphere is opaque at wavelengths below 300 nm. "To take advantage of this optical window, Earth to space communication requires detectors that are UV sensitive, but blind to the ambient visible radiation" [3]. Other applications include medical imaging (280-400 nm), protein analysis and DNA sequencing (240-300 nm), forensic analysis (250-300 nm) [1].

Today, there is a wide variety of detectors available to detect ultraviolet radiation. Traditionally, photomultiplier tubes have been attractive, but they require bulky vacuum based components. Large band gap materials like AlGaN, diamond, and ZnO can be used to make visible-blind, and solar-blind ultraviolet detectors. However, they are difficult to grow/deposit in high purity, uniform layers, to dope in controlled and/or to process at large areas with low costs. Silicon detectors with ultraviolet band pass filters are the most common, and low cost commercial solutions available for ultraviolet detection. But, they suffer from intrinsically low responses in the ultraviolet, limited lifetimes due to degradation under prolonged ultraviolet exposure, and difficulties in fabricating the necessary filters [9]. Alternatively, lumogen has been used to downshift the ultraviolet light. However, the lumogens have few disadvantages. The light emission is over a broad spectrum, and they tend to degrade with time, ultraviolet and vacuum exposure. Also, the device users have also reported uniformity problems, and pin holes development when used in vacuum.

2.2 Introduction of UV Detectors

Ultraviolet detector is an optoelectronic device that absorbs optical energy in UV region and converts it to electrical energy, or generates a chemical reaction. It detects the light spectrum beyond violet, which is invisible to human eye. An ideal ultra violet photo detector has a high responsivity, and sensitivity. It shows good linearity of photocurrent as a function of the incident optical power. It exhibits high spectral selectivity, low noise level, and short response time. The type of application determines the priority given to the above mentioned characteristics. For example, a short response time is crucial for UV imaging applications where it is important to quickly process real time data [2]. The fig. 2-1 categorizes the state of the art ultraviolet detectors.

Responsivity, sensitivity, and noise equivalent power are figures of merit of these detectors. Responsivity is defined as the RMS signal voltage or current at the output of the detector per unit optical input signal power. Sensitivity of a detector determines the minimum signal it can detect. Noise equivalent power (NEP) is defined as the radiant input signal power that yields a signal to noise ratio of unity at the output.

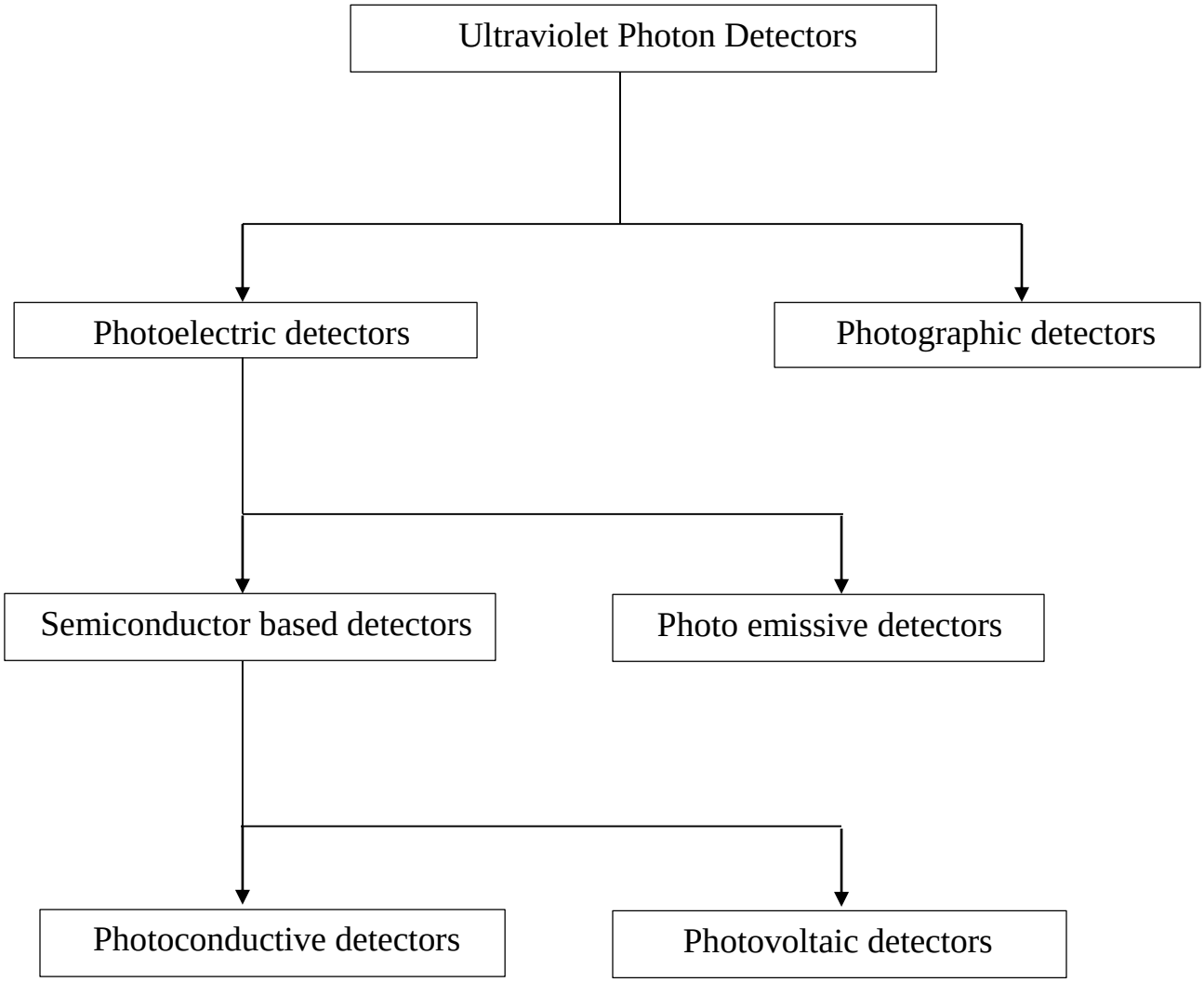

Fig. 2-1. Classification of UV detectors [1].

2.3 Photographic Detectors

In a photographic detector, an incoming photon generates a chemical reaction, and the image is further developed. They are used for their image storing capability, and large amounts of data storage in single exposure. However, there are few drawbacks associated with photographic detectors. The sensitivity of photographic detector is lower than the photoelectric detector. The dynamic range is limited, the response is not a linear function of the incident photon flux, and it has low operational speed.

2.4 Photoelectric Detectors

In a photoelectric detector, incident light is detected by measuring the generated electrical signal. They can be divided into two types of detectors- photo emissive detectors and semiconductor detectors.

2.4.1 Photo emissive Detectors

The photo emissive detectors utilize the photoelectric effect to detect ultraviolet light. The photoelectric effect is the phenomena in which electrons are released from the material when the incident light energy is more than the work function of the material. The most common configuration allows the photon to impact a solid surface; releasing a photoelectron into the vacuum environment. The voltage is applied between the photocathode surface and a positively biased anode, which causes a photoelectron to flow in proportion to the intensity of the incident radiation. The fig. 2-2 shows the operation of

photo emissive detector. The wavelength range of sensitivity is defined primarily by the work function of the surface material. The primary photoelectron can be multiplied by the process of secondary emissions to produce a large cloud of electrons. The degree of multiplication is called the gain of the detector. Based on the gain, it can either be detected with conventional electronic circuits or accelerating it to high energy, and then recording the impact on phosphor screen. For a single photon detection, one has to resort to photo emissive detectors as they offer highest detection sensitivity at low noise. However, they are bulky and cumbersome to carry. It is not possible in this mode of operation to store the detected events in the detector. They have low quantum efficiency, and strong spectral dependence of responsivity. The sensitivity of photocathode surface to surface contaminants is also an issue [3].

2.4.2 Semiconductor UV Detectors

The photons are absorbed in the bulk of the semiconductor material producing electron-hole pairs which are separated by an electric field. The minimum energy required to excite an electron from valence band to conduction band is equal to the band gap of the material. The wavelength corresponding to the minimum energy is called the cut-off wavelength. They are divided into two categories- photoconductive detectors and photovoltaic detectors.

Photoconductive detector is the simplest optical detector that exhibits an internal gain mechanism, and clearly demonstrates the gain-bandwidth limitation. It can also be

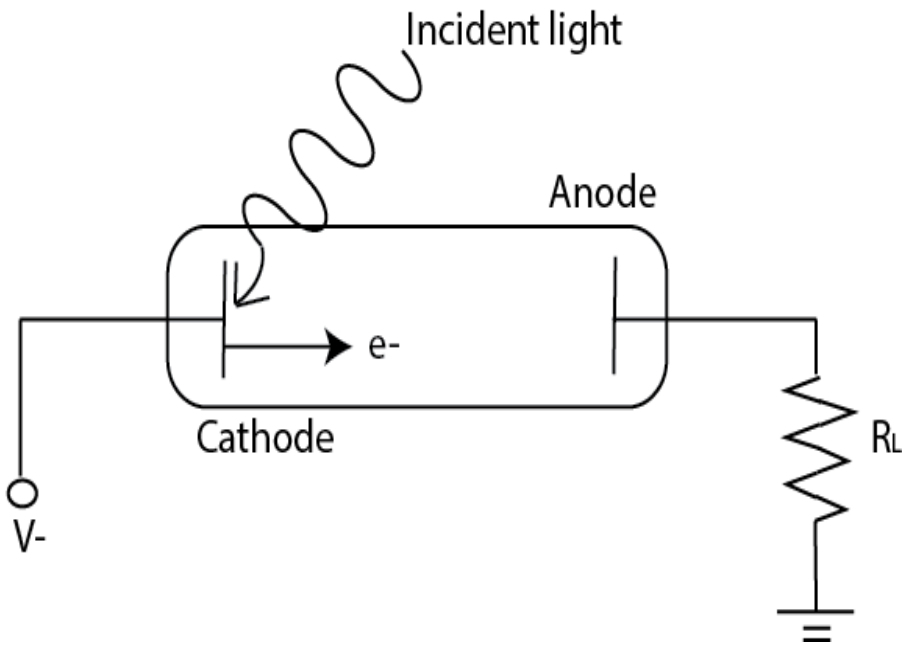

Fig. 2-2. Photo emissive detector.

stated as a ‘radiation sensitive resistor’. It detects light by measuring the increase in conductivity of the sample with photo excitation. The photo generated electrons and holes are collected by opposite contacts, and result in a photocurrent. A suitable bias is applied across the contacts to collect the photo generated carriers. Depending on the resistance, they are operated in two configurations. First, for low resistance material, it is operated in a constant current circuit. The series load resistance is large compared to the sample resistance, and the signal is detected as a change in voltage developed across the sample. Second, for high resistance material, a constant voltage is preferred and the signal is detected as a change in current in the bias circuit. The fig. 2-3 shows an illustration of a photoconductive detector.

The photon detection in structures with built-in potential barriers are essentially photovoltaic. It is a junction device which uses the internal electric field to move electrons and holes in opposite directions. They are commonly used in four different structures - p-n homo junction, p-i-n diode, p-n hetero junction and schottky barrier.

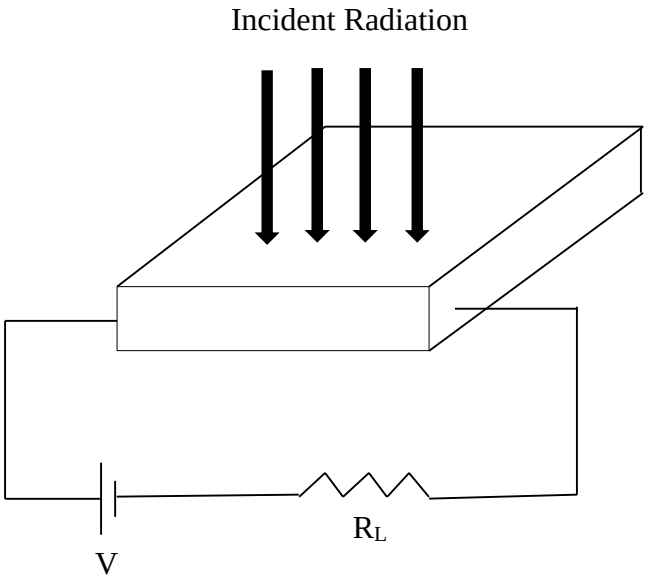

Fig. 2-3. Illustration showing photo conductive detector.

2.5 Photovoltaic Detector

The junction photodiode is the most common photo detection device that is used both in ordinary, and specialized applications. It is often referred to simply as a photodiode. They can be made with any semiconductor material in which a p-n junction can be formed. The basic principle of operation of a junction photo diode is very simple. The diode is operated under reverse-biased conditions to increase the depletion width. Under reverse bias conditions, a small dark current, called as the reverse saturation current flows through the device. When the light is incident on the homo-junction photodiode, photons are absorbed mainly in the depletion region and also in the neutral regions, particularly on the top, where the light is incident. The absorbed photons create electron-hole pairs. The photo generated carriers in the depletion region are accelerated in opposite directions by the internal electric field. It gives rise to the photocurrent, the magnitude of which depends on the quantum efficiency. The carriers that are produced within a diffusion length of the depletion layer, on either side of it, also reach the depletion region by diffusion and are then accelerated by the internal electric field, thereby contributing to the photocurrent. Therefore, photo excitation is detected as an increase in the reverse biased current of a junction photodiode [9]. Fig. 2.4 shows an illustration of a p-n junction, and its band diagram.

The following lines give the mathematical equations of a p-n junction diode. The total current density is usually written as [10]:

$$J(V,\Phi) = J_d(V) - J_{ph}(\Phi),$$

where the dark current density J_d, depends only on V, and the photocurrent depends only on the photon flux density Φ.

The magnitude of photocurrent density is given by [11]:

$J_{ph} = \eta q \Phi$,

where η is the quantum efficiency.

The dark current is given by [12]:

$J_d = J_s (\exp(qV/kT)-1)$,

where reverse saturation current density (Js) is equal to [13]:

$J_s = qD_h p_{no}/L_h + qD_e n_{po}/L_e$,

D_h and D_e are the hole and electron diffusion coefficients respectively, while L_h and L_e are the hole and electron diffusion length respectively.

If the p-n diode is open circuited, the accumulation of electrons and holes on the two sides of the junction produces an open-circuit voltage. If a load is connected to the diode, a current will conduct in the circuit. The maximum current is realized when an electrical short is placed across the terminals, and this is called the short-circuit current [3]. The fig. 2-5 shows the equivalent circuit diagram of an illuminated photodiode and its current voltage characteristics.

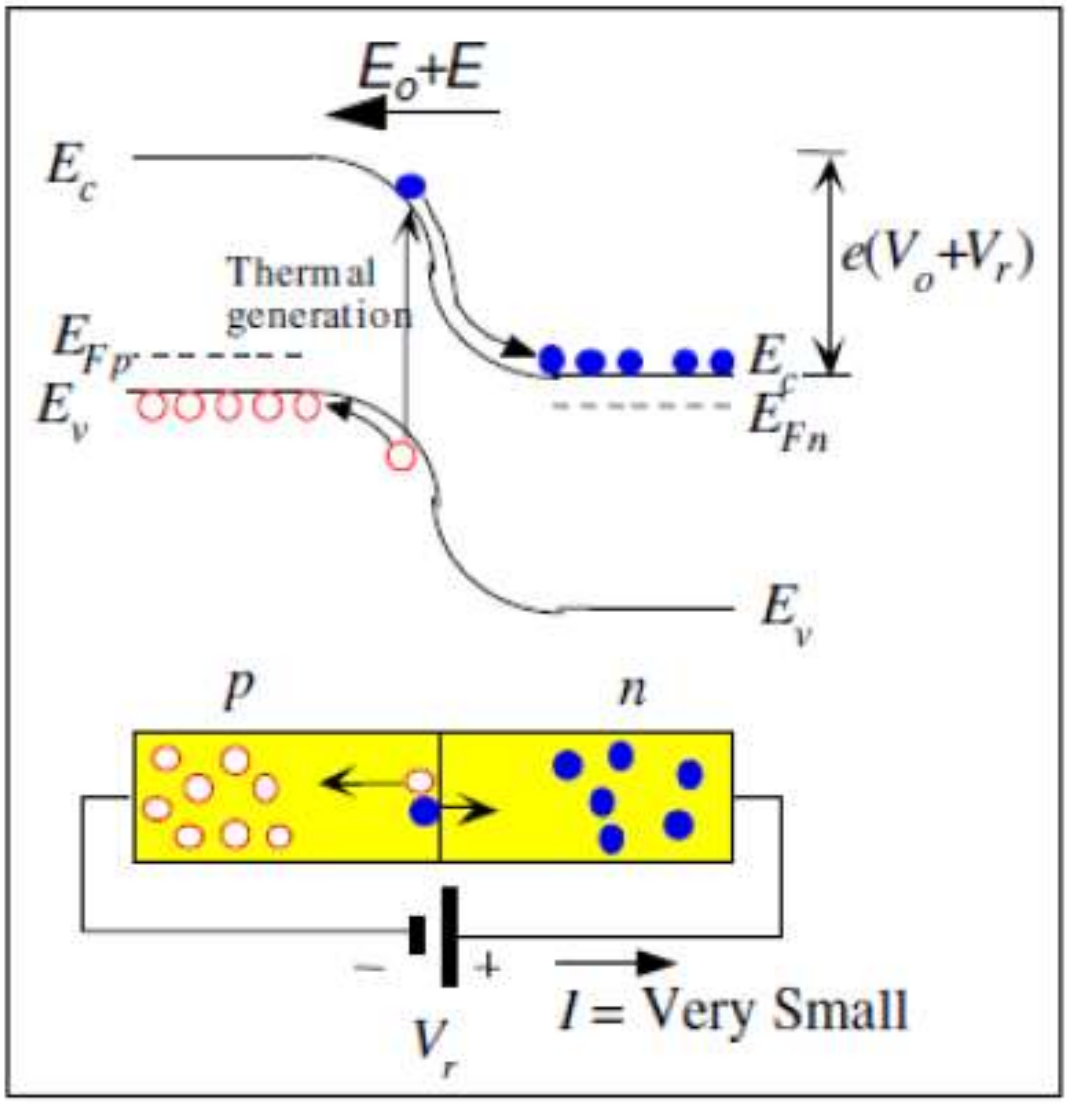

Fig. 2-4. Band diagram of a p-n homo junction photo diode, and its operation [14].

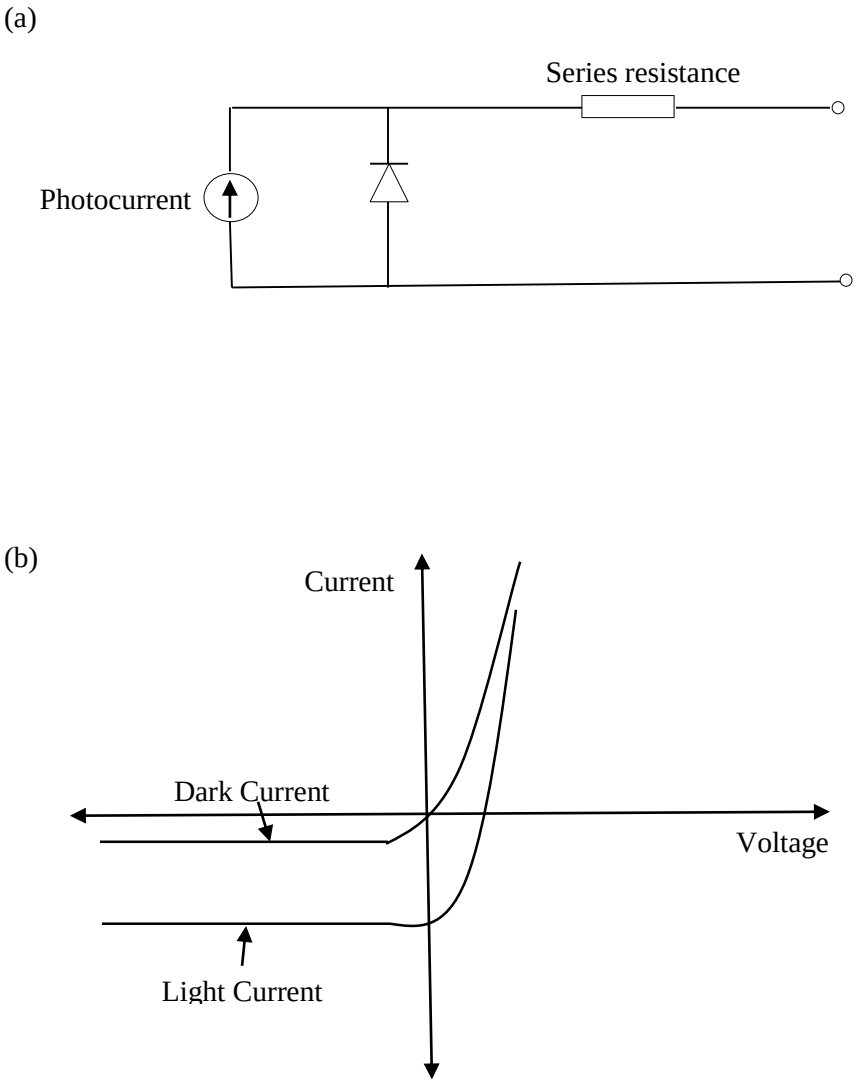

Fig. 2-5. (a) Equivalent circuit of an illuminated photodiode. (b) Current-voltage characteristics of an illuminated and non-illuminated photodiode.

2.6 Luminescent Downshifting Materials

Luminescent down-shifting (LDS) refers to the absorption of short wavelength incident photons, and their re-emission at longer wavelengths. The fig. 2-6 shows the mechanism of luminescent down-shifting. LDS is a passive approach that involves application of luminescent species over the cell, thus eliminating the need to interfere with the active material of the photovoltaic device. The luminescent species should ideally exhibit unity luminescent quantum efficiency (LQE), which is defined as the ratio of the number of photons emitted to the number of photons absorbed by the luminescent species. They should have a wide absorption band in the region where the external quantum efficiency (EQE) of the cell is low, and a high absorption coefficient. The narrow emission band should also coincide with the peak EQE of the cell. In order to minimize losses due to re-absorption, the absorption and emission bands should be well separated. Low cost and prolonged photo stability for periods of 20-25 years are other important characteristics of an ideal luminescent species [15].

LDS materials can be separated into three main categories: quantum dots, organic dyes, and rare earth ions/complexes. The organic dyes exhibit relatively high absorption coefficients [16], close to unity LQE [17], and are easy to process in polymeric materials. However, they have narrow absorption bands, and relatively small Stokes-shift, which still results in significant reabsorption losses [18]. Although, significant improvements have been reported in recent years, but still the photo stability remains questionable [17]. The rare-earth ions exhibit relatively high LQE, but they suffer from low absorption

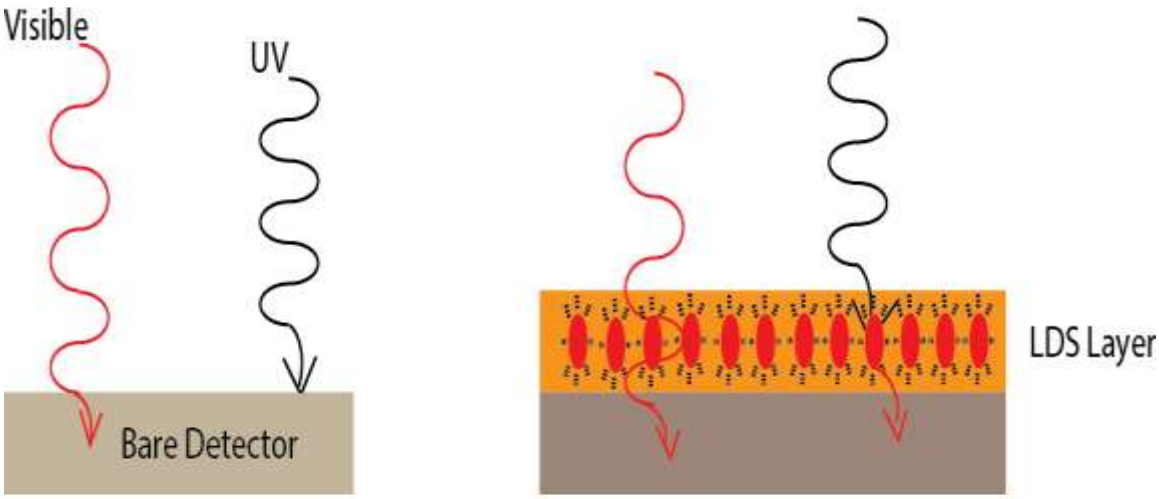

(a) (b)

Fig. 2-6. Sketch of quantum dot sensitized UV detector. (a) Visible light (red curved line) is collected in the active region, UV light (black curved line) is collected near the surface of the bare detector. (b) UV light is absorbed by red quantum dots and re-emitted in the visible region.

coefficients. On the other hand, quantum dots exhibit a wide absorption band, high emission intensity, and relatively good photo stability [19].

2.7 Quantum Dots

A semiconductor material whose excitons are spatially confined in all three dimensions is called a quantum dot [20]. When the size of the quantum dot is smaller than the critical characteristic length, which is called the exciton Bohr radius, then the quantum confinement effect starts dominating. The states of the exciton shift to higher energy as the confinement energy increases. The increase in confinement energy is in agreement with the Heisenberg uncertainty principle, i.e. the momentum of a particle increases if its position becomes well defined. In the limit of small particles, the strongly screened coulomb interaction between the electron and hole can be neglected. Therefore, both the electrons and holes can be described by a particle in the box model, which leads to discrete energy levels that shift to higher energies as the box is made smaller [21].

Cadmium selenide quantum dots were chosen in this study, because of their fluorescence in the visible region. For semiconductor nano crystals, it is found that in naked particles, surface effects created by chemical reactions or surface reconstruction are detrimental for achieving a high luminescence quantum yield. Any surface defect will lead to allowed electronic states in the gap region. Consequently, non-radiative relaxation pathways involving trap states become predominant. This leads to a dramatic reduction of the luminescence quantum yield. In order to avoid the surface defects, nano crystals are usually capped with a protective layer of a second larger band gap semiconductor, which

is ZnS capping layer in CdSe case. With this protective shell, it is possible to functionalize the particles by applying suitable surface chemistry without interfering with the optical properties [21]. The fig. 2-7 represents an illustration of CdSe/ZnS quantum dot, and the band diagram of CdSe/ZnS core-shell quantum dot.

2.7.1 Physics of Quantum Dots

The density of allowed energy states (D(E)) as a function of energy tells us about the number of available quantum states. It is used to determine the electron and hole concentrations. The density of states as a function of energy differs for bulk (3D), quantum well (2D), quantum wire (1D) and quantum dot (0D). The fig. 2-8 shows an increasing order of confinement of a material in three dimension, with their density of states as a function of energy. The shape of the curve of density of states with energy depends on the degree of confinement. The table 2-1 relates the density of states with degree of confinement.

According to Pauli's exclusion principle only two electrons with different spins can occupy the same energy level. The density of states in a quantum dot is expressed as a delta-function, and the integration of electron density gives two electrons in a certain quantum level.

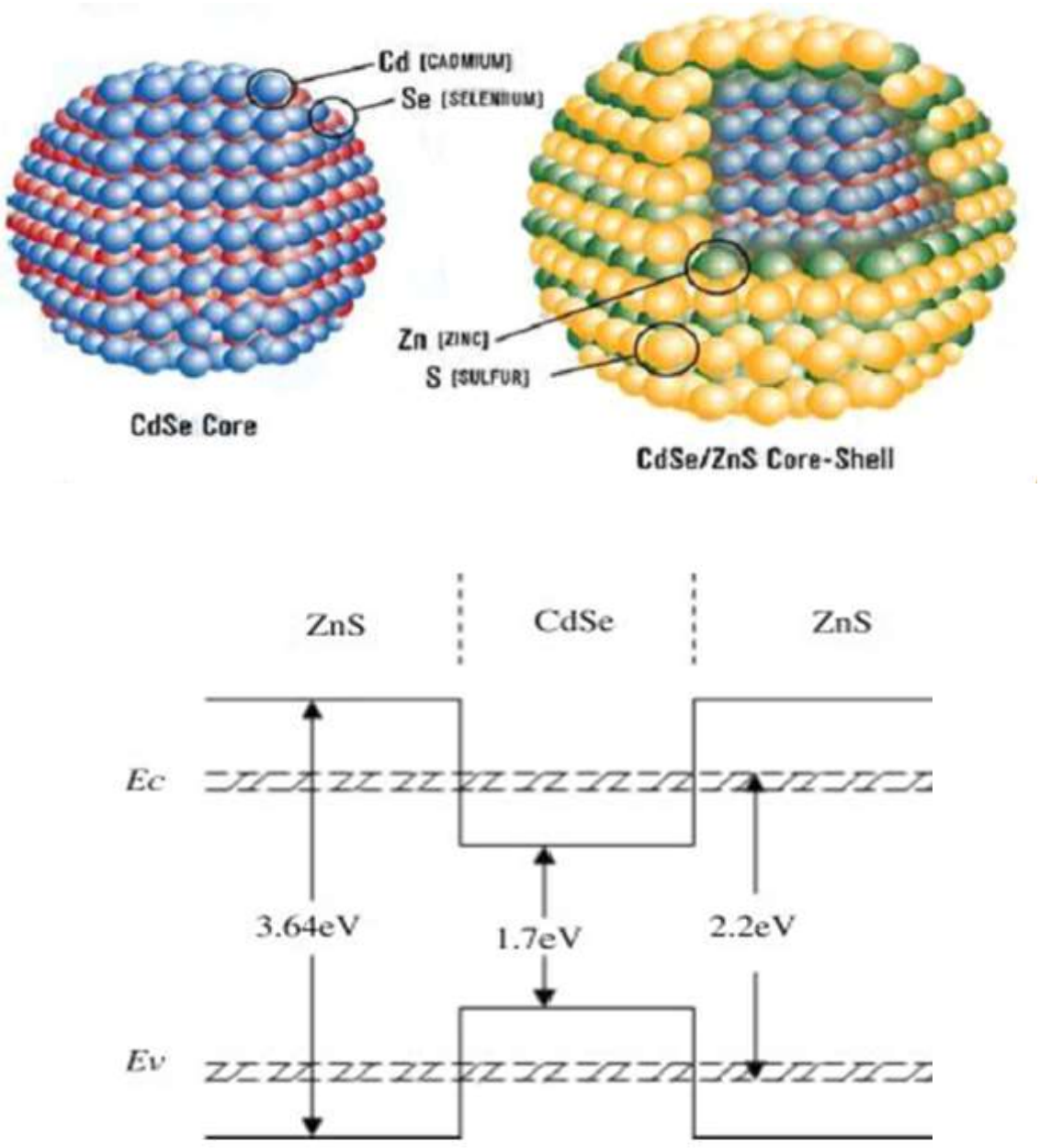

Fig. 2-7. (a) Illustration of CdSe core and CdSe/ZnS core-shell quantum dot. (b) Band diagram of CdSe/ZnS core-shell quantum dot [22].

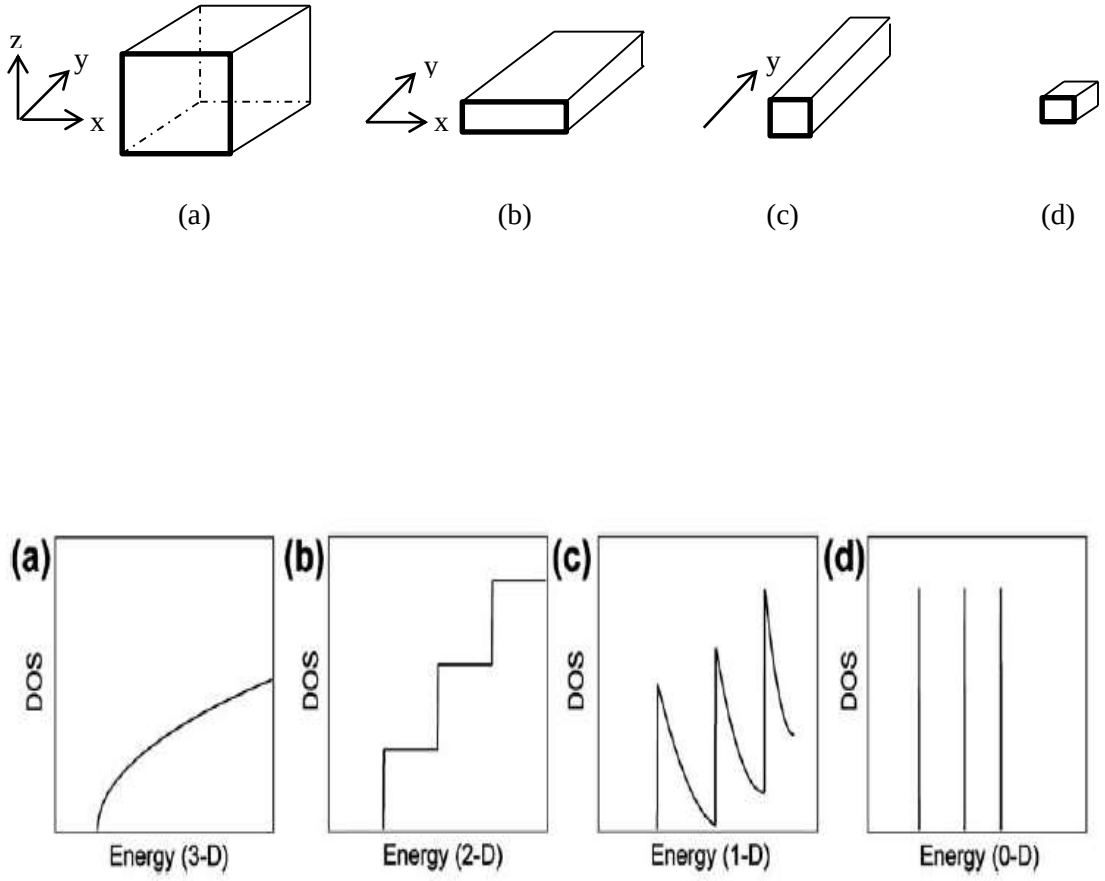

Fig. 2-8 Schematic illustration of the density of states as a function of energy for: (a) a bulk material (3-D), (b) a quantum well (2-D), (c) a quantum wire (1-D), (d) a quantum dot (0D) [23].

Table 2-1 Density of states of semiconductor material [24].

Structure	Confinement	Density of States
Bulk	0D	$N(E) = \frac{m^* \sqrt{2m^* E}}{\pi^2 \hbar^3}$
Quantum Well	1D	$N(E) = \frac{m^* i}{\pi \hbar^2 L_x}$
Quantum Wire	2D	$N(E) = \frac{\sqrt{2m^*}}{\pi \hbar L_x L_y} \sum_{i,j} \left(E - E_{i,j}\right)^{-\frac{1}{2}}$ where $E_{i,j} = \frac{\hbar^2 \pi^2}{2m^*} \left(\frac{i^2}{L_x^2} + \frac{j^2}{L_y^2}\right)$
Quantum Dot	3D	$N(E) = \frac{2}{L_x L_y L_z} \sum_{i,j,k} \delta(E - E_{i,j,k})$ where $E_{i,j,k} = \frac{\hbar^2 \pi^2}{2m^*} \left(\frac{i^2}{L_x^2} + \frac{j^2}{L_y^2} + \frac{k^2}{L_z^2}\right)$

According to the effective mass approximation model [25], the effective band gap of a nanoparticle is given by:

$$E^*(r) = E_g^{bulk} + \frac{\hbar^2\pi^2}{2er^2}\left(\frac{1}{m_e^*} + \frac{1}{m_h^*}\right) - \frac{1.8e}{4\pi\epsilon\epsilon_o r} - \frac{0.124e^3}{\hbar^2(4\pi\epsilon\epsilon_o)^2}\left(\frac{1}{m_e^*} + \frac{1}{m_h^*}\right)^{-1}$$

where,

E^* is the effective band gap of the quantum dot,

E_g^{bulk} is the bulk band gap of the material,

r is the radius of the nanoparticle,

m_e and m_h are the effective masses of electrons and holes respectively, and ϵ is the dielectric constant of the material.

The second term on the right side of the equation represents an increase in energy due to particle in a box confinement. The third term represents a lowering of energy due to electron-hole interaction via shielded coulomb interaction mechanism. The fourth term, negligibly small and size dependent, is a polarization term and accounts for spatial correlation [26].

In quantum dots, the electronic states can be understood as confined states in atoms or molecules where electrons are bound in discrete energy levels forming a 3-D confinement potential. The separation between the highest occupied molecular orbital (HOMO) and the lowest unoccupied molecular orbital (LUMO) is considered the band gap of the quantum dot.

The fig. 2-9 illustrates the variation in band gap with the size of quantum dot. The band gap of quantum dot increases with decrease in size.

2.7.2 Fluorescence properties

Fluorescence is a form of luminescence where the emitting light has a longer wavelength than the absorbed light or electromagnetic radiation. It is the result of a three-stage process that occurs in certain molecules (generally poly aromatic hydrocarbons or hetero cycles) called fluorophores or fluorescent dyes. It is a three step process: excitation, excited-state lifetime, fluorescence emission. The fig. 2-10 shows the three steps of fluorescence.

In the first process, a photon of energy $h\nu_{EX}$ is supplied by an external source of light, and absorbed by the fluorophore, creating an excited electronic singlet state (S_1'). This process distinguishes fluorescence from chemiluminescence, in which the excited state is populated by a chemical reaction [28].

The excited state has a finite lifetime, typically 1–10 nanoseconds. During this time, the fluorophore undergoes conformational changes, and is also subjected to a multitude of possible interactions with its molecular environment. These processes have two important consequences. First, the energy of S_1' is partially dissipated, yielding a relaxed singlet excited state (S_1) from which fluorescence emission originates. Second, not all the molecules initially excited by absorption (Process 1) return to the ground state (S_0) by fluorescence emission. Other processes, such as collisional quenching, fluorescence resonance energy transfer (FRET), and intersystem crossing may also depopulate S_1. The fluorescence quantum yield, which is the ratio of the number of fluorescence photons emitted to the number of photons absorbed, is a measure of the relative extent to which these processes occur [28].

In the final step, a photon of energy $h\nu_{EM}$ is emitted, returning the fluorophore to its ground state S_0. Due to energy dissipation during the excited-state lifetime, the energy of this photon is lower, and therefore, photons of longer wavelength, than the excitation photon $h\nu_{EX}$. The difference in energy or wavelength represented by ($h\nu_{EX} - h\nu_{EM}$) is called the Stokes shift. Fig. 2-10 (a) shows the three step process of fluorescence [28].

The fig. 2-10 (b) shows the normalized fluorescence intensity v/s wavelength. The fluorescence intensity maximum shifts to longer wavelengths with the increase in size of quantum dots. Since, the band gap reduces with increase in the size of quantum dots, the bigger size quantum dots will fluoresce at longer wavelengths.

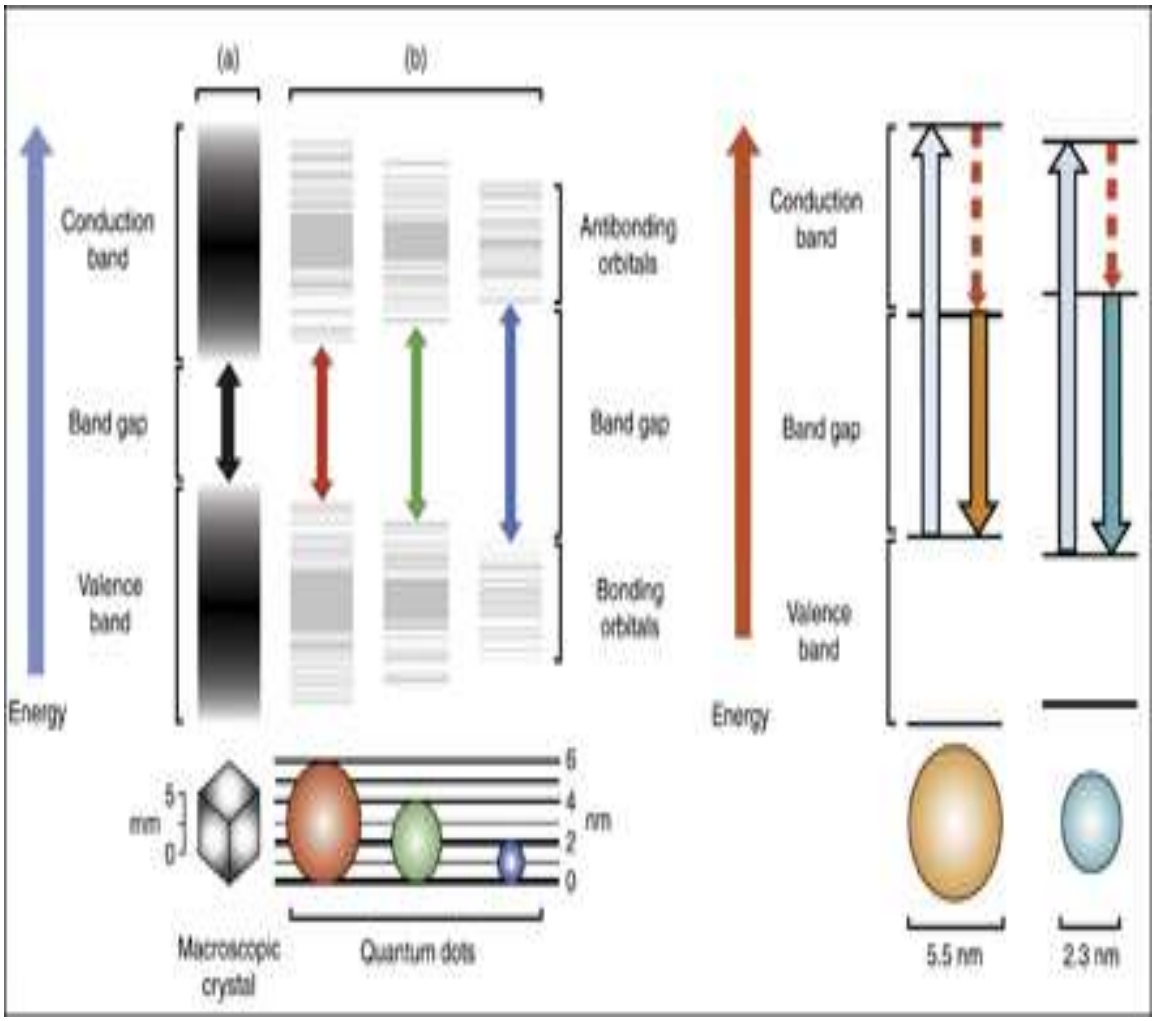

Fig. 2-9. Illustration showing variation of band gap with size [27].

(a)

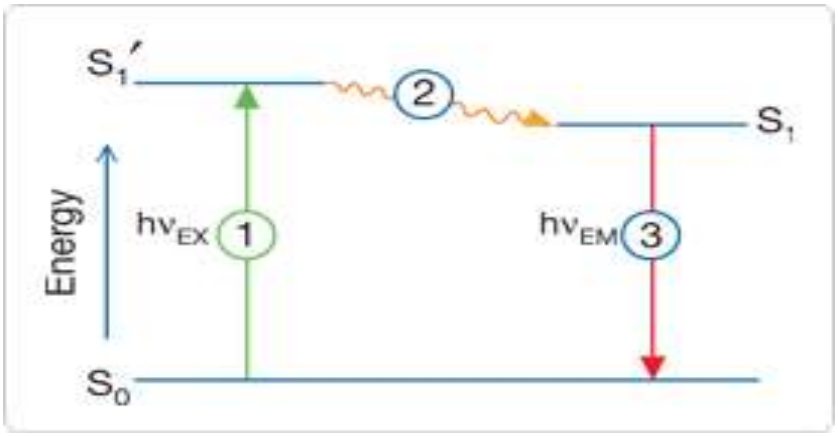

(b)

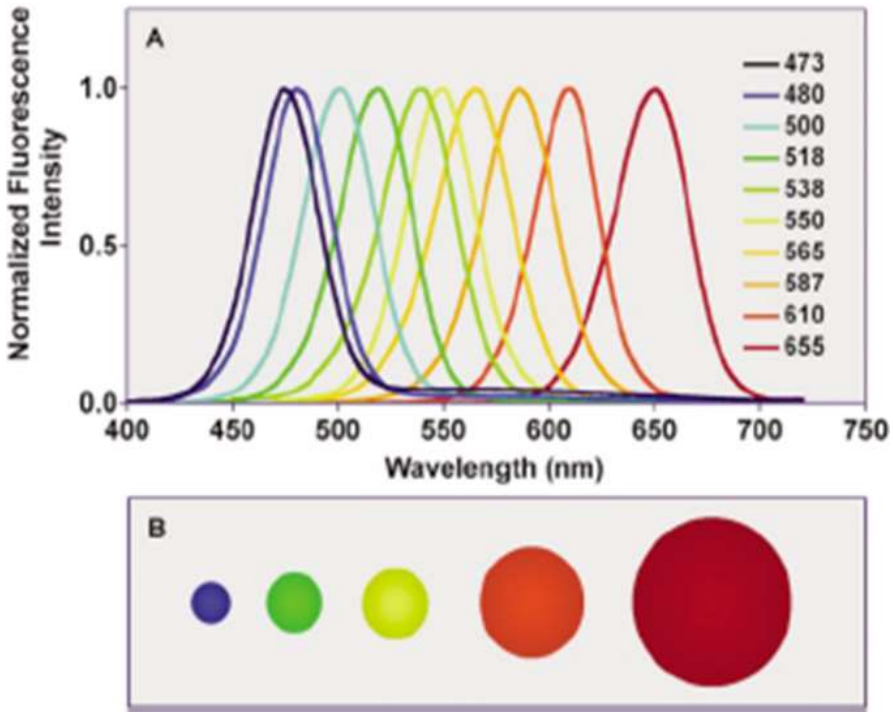

Fig. 2-10. (a) Sketch showing the phenomena of fluorescence [28]. (b) Normalized fluorescence intensity of CdSe/ZnS with increase in size of quantum dots [29].

2.8 Mist Deposition

It is a physical liquid deposition method, used primarily to deposit films as thin as few mono layers. The fig. 2-11 shows the schematic of the mist deposition tool. The liquid precursor solution flows into the atomizer by Venturi effect. The venture type nozzle converts the liquid solvents into fine droplets. The carrier gas, ultrapure nitrogen, carries the solvent droplets through chambers of the atomizer. Fig. 2-12 shows the internal structure of the atomizer. The impactors in the atomizer separate the droplets according to the size, which is based on the inertia of the droplets. Larger droplets hit the impactors, and settle down into the chamber in liquid form; while, the smaller droplets are carried into subsequent chambers, and finally to the deposition chamber. The selected drop size depends on the viscosity and density of the solvent, and it is quarter micron for toluene which is used as a solvent for this study. At this size, the gravity effects are not sufficient to settle the drops and they remain suspended in the atomizer in the form of a mist, giving the process its characteristic name. The carrier gas carriers the mist to the deposition chamber. The mist is believed to be charged at the point of generation, due to shearing forces from the carrier gas. Overall, the mist is neutral, with equal number of positively and negatively charged mist.

The mist remains suspended in the chamber and gets attracted to the substrate by the application of electric field between the field screen and the substrate. The flow of mist is uniform and laminar. Under the action of electric field, the negatively charged mist is deposited on the substrate. This limits the precursor usage efficiency inside the chamber, though, most of the loss takes place inside the atomizer during the size selection.

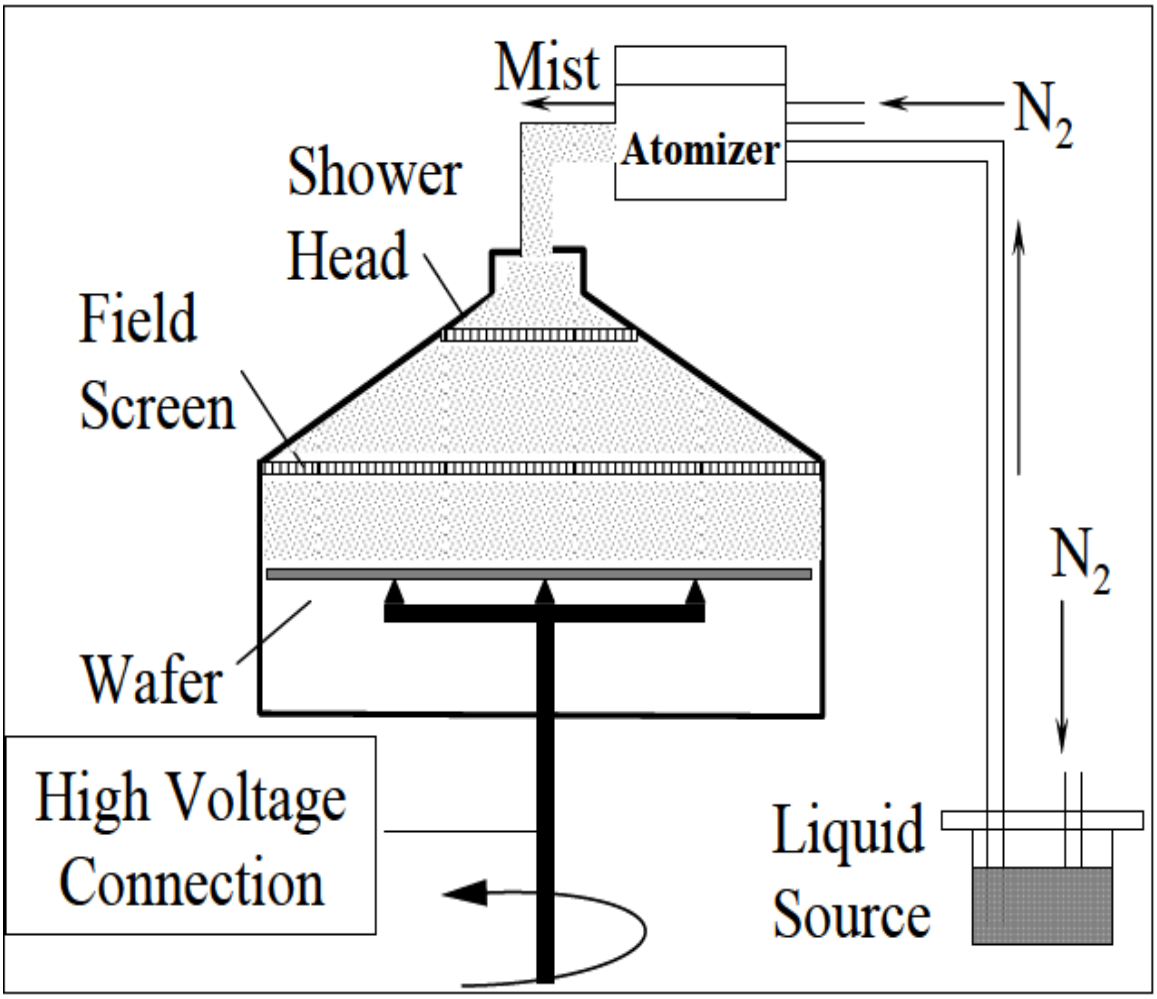

Fig. 2-11. Schematic of mist deposition system [30].

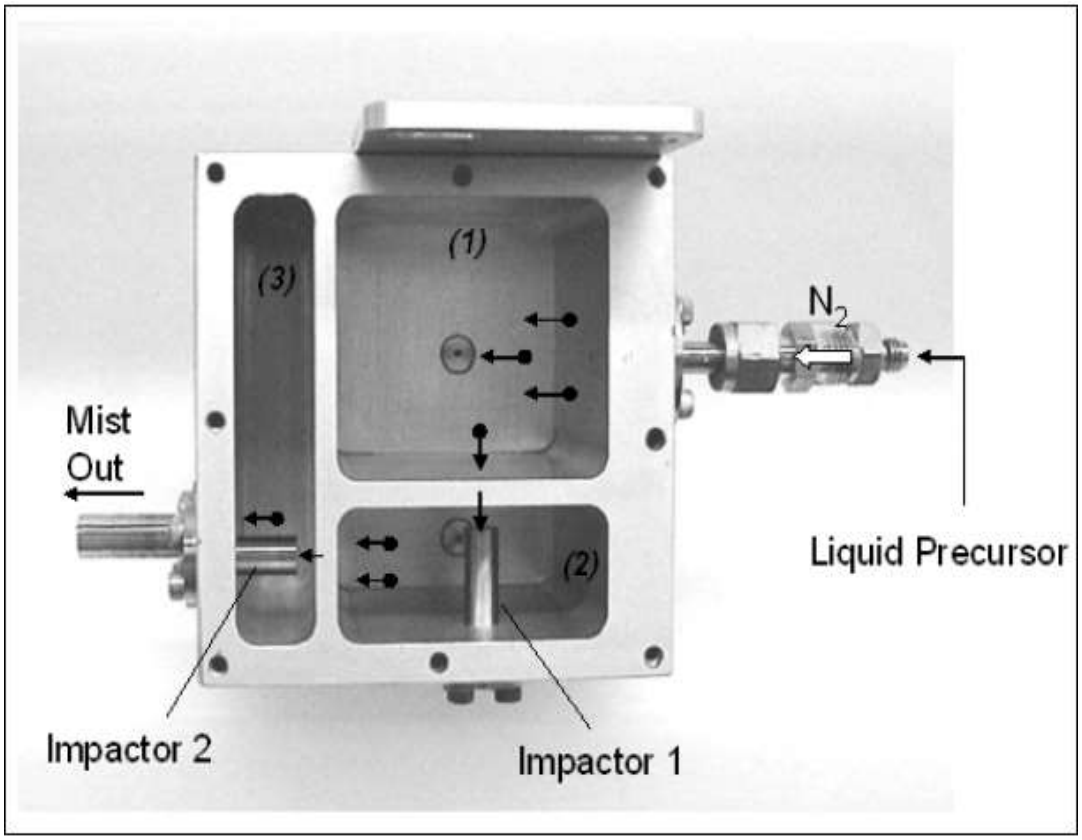

Fig. 2-12. Internal structure of atomizer [26].

Finally, the solution left behind in the atomizer can be easily recovered and reused.

2.9 Sources of UV

The sun is the primary source of ultraviolet radiation. It emits UV at all wavelengths, including extreme UV. The solar constant output of sunlight in space, at the top of Earth's atmosphere is about 1366 W/m^2. The total energy is composed of about 50% infrared light, 40% visible light, and 10% ultraviolet light, for a total ultraviolet power of about 140 W/m^2 in vacuum [31]. However, most of the shorter wavelength (below 300 nm) UV is blocked by earth's atmosphere. Apart from the sun, there are other artificial sources of ultraviolet light. Black light is a lamp that emits long-wave UV A radiation, and little visible light. They are constructed as normal fluorescent lights, except they use a phosphor on the inner tube surface, which emits UVA light instead of visible white light. Short wave ultraviolet lamps are also made by using fluorescent lamps without an internal phosphor coating. They emit ultraviolet light with two peaks in the UV-C band at 253.7 nm, and 185 nm, due to the peak emission of mercury within the lamp. Specialized UV gas-discharge lamps are sold, containing a variety of different gases, to produce UV light at particular spectral lines for scientific purposes. Argon and deuterium lamps are often used as stable sources, either windowless or with various windows, such as magnesium fluoride [32]. In the last two decades, excimer (short form for excited dimer) lamp is seeing increasing use in scientific fields. It has the advantages of high intensity, broadband radiation, and operation at a variety of wavelength bands into the vacuum ultraviolet. Recent development in GaN based light emitting diodes (LED's), allows them to emit light in the ultraviolet

range. But, the LED's efficiency at 365 nm is only 5-8%, while it improves for longer UV wavelengths, for 395 nm it is close to 20%. UV gas lasers, laser diodes and UV solid-state lasers are also common sources of UV light. The nitrogen gas laser uses electronic excitation of nitrogen molecules to emit UV, with strongest lines at 337.1 nm. Excimer laser is another type of high power gas laser. They emit in ultraviolet, and even vacuum ultraviolet wavelength range. Direct UV emitting laser diodes are available at 375 nm. Diodes in solid-state module use frequency doubling or tripling diode-pumped solid state technology to generate wavelengths shorter than 325 nm [33].

2.10 Applications of UV

Ultraviolet light has a huge number of applications in modern society. It is important because of its ability to cause chemical reactions and excite fluorescence in materials. Table 2-2 lists the application of specific wavelength bands in UV spectrum.

Table 2-2 Applications of UV [33].

Wavelength (nm)	Application
13.5	Extreme UV lithography
30-200	Photoionization, UV photoelectron spectroscopy
230-365	UV-ID, label tracking, barcodes
230-400	Optical sensors, various instrumentation
240-280	Disinfection, decontamination of surfaces and water
200-400	Forensic analysis, drug detection
270-360	Protein analysis, DNA sequencing, drug discovery
280-400	Medical imaging of cells
300-320	Light therapy in medicine
300-365	Curing of polymers and printer inks
300-400	Solid-state lighting
350-370	Bug zappers

Chapter 3

Scope and Objectives

The detection of ultraviolet radiation has been of great interest for industrial, medical, military, and environmental applications. The limited spectral response of the silicon detectors to the shorter wavelengths has resulted in the research of luminescent downshifting materials. Quantum dots have shown a great promise as a luminescent downshifting material. The luminescent downshifting layer has shown improvement in the spectral response of the detectors by down-shifting the short wavelength light. The impact is not only limited to the detectors, but also to the photovoltaic industry making commercial solar cells.

As stated earlier, quantum dots offer useful advantages as luminescent downshifting materials. Physical liquid deposition techniques are the most promising techniques to deposit these materials. Out of these techniques, mist deposition allows the controlled deposition of ultra-thin films of quantum dots on planar as well as circular substrates.

The objective of this study was to demonstrate the down-shifting principle to improve the poor spectral response of silicon detectors to short wavelength light. The luminescent downshifting layer of quantum dots absorbs photons, typically in the 300-500 nm range, and re-emits them at a longer wavelength (620 nm), which is close to the peak

sensitivity of silicon. Mist deposition tool was used to deposit ultra-thin films of quantum dots, making the use of quantum dots cost effective.

Chapter 4

Experiment

This chapter outlines the various experiments performed during this study. It shows the design of the device, and the experimental setup used for this device. In this study, two types of detector configurations were used, i.e. photoconductive and photovoltaic. Different contact configurations were tried using shadow masks in the photoconductive detector design, while a commercial photodiode was used for the photovoltaic configuration.

4.1 Liquid Precursors

The CdSe/ZnS core-shell quantum dots used in this study have a peak fluorescence at 620 nm, with a quantum yield of 91%, and were provided by Evident Technologies Inc. in a colloidal solution. The colloidal solution of quantum dots in toluene was specified in terms of optical density, and was 0.16 for red quantum dots.

4.2 Mist Deposition

Mist deposition was used to deposit ultra-thin layers of quantum dots on the test structures. The carrier gas supply, ultrapure (>99.99%) nitrogen, was maintained at a pressure of 60 psi. The flow rate of 2ml/min was maintained for every experiment. Experimental variation

was mainly carried out by changing the deposition time. The deposition time of 5, 10 and 20 minutes was used for this study.

4.3 Photoconductive Detector

The silicon photoconductive configuration was realized by making ohmic contacts to the silicon wafer. A p-type silicon wafer, <100> orientation, with a doping concentration of $3.12*10^{15}/cm^3$ was used. Aluminum was selected as a choice of metal to make ohmic contacts. The physical vapor deposition technique was used to deposit the aluminum using aluminum clips, purity of 99.99%. Different shadow masks were used to pattern the contacts to give different test structures. Fig. 4-1 shows the different test structures used in the study. The contact area of rectangular contacts was 298.57 mm^2, and for circular contacts it was 7.20 mm^2

The current-voltage characteristics were measured using the Keithley 237 High Voltage Source Measure Unit. LABVIEW 7.1 was used to control the operation of voltage source. The DC voltage was swept from -6 to 6V. The light source used in this experiment was UV Lamp Model UVL-56 (Black-Ray Lamp). The wavelength emitted is long wave UV-365 nm. The distance between the UV lamp and the sample was 5 cm.

(a)

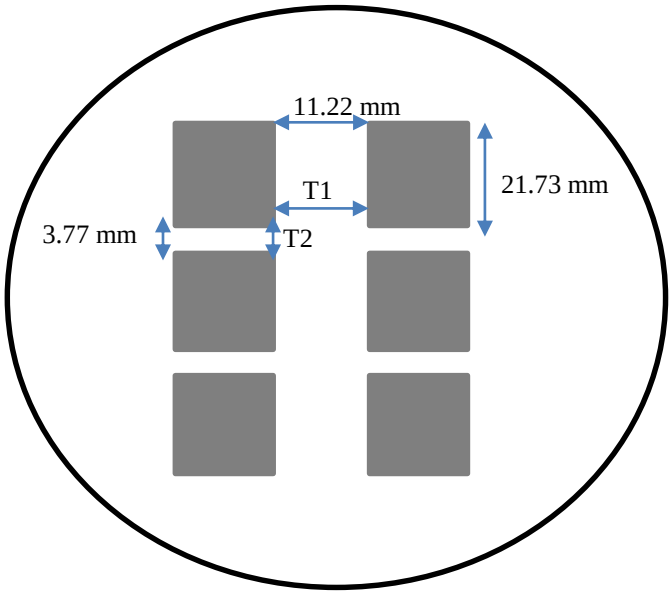

(b)

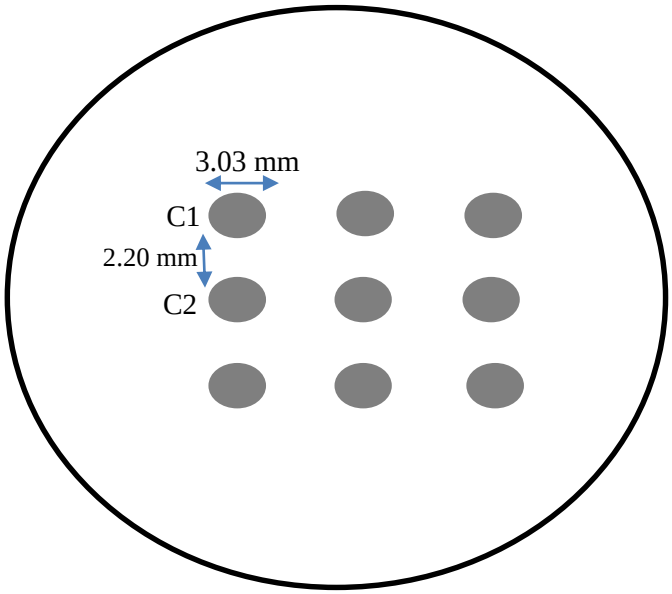

Fig 4-1. (a) Test structure I with rectangular contacts. (b) Test structure II with circular contacts.

4.4 Photovoltaic Detector

The planar silicon photodiode from Silonex Inc. was used in this study. Fig. 4-2 shows the sketch of the UV detector. The external quantum efficiency measurements were taken by Princeton Instruments, Acton SP2150 equipped with a xenon arc lamp to generate monochromatic light from 300 to 1100 nm. The incident power was measured using a calibrated Newport 818-UV enhanced silicon photodiode. Long pass color filter FGL550S from Thor Labs Inc. was used to isolate the monochromatic light. Keithley 2401 Source Meter was used to measure the current-voltage characteristics of the photodiode. The light source used in the experiment was 40mW laser from ONDAX Inc., with an emission wavelength of 405 nm.

(a)

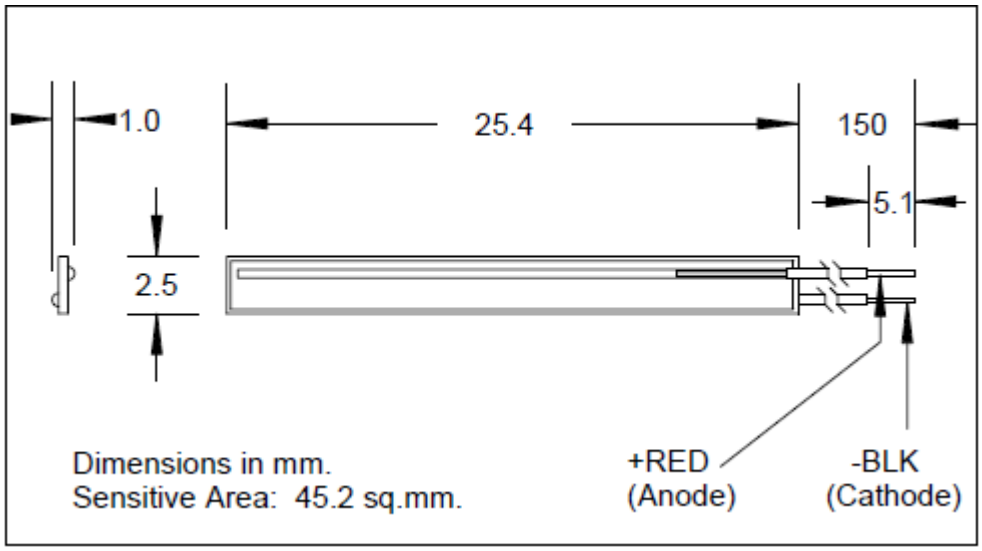

(b) (c)

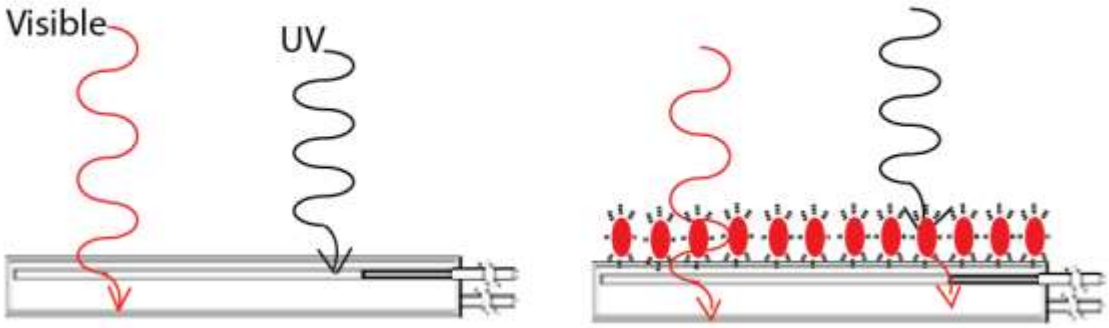

Fig. 4-2. Sketch of quantum dot sensitized UV detector. (a) Silicon planar photodiode from Silonex Inc. used in this study. (b)Visible light (red curved line) is collected in the active region, UV light (black curved line) is collected near the surface of the bare detector. (c) UV light is absorbed by red quantum dots and re-emitted in the visible region.

Chapter 5

Results and Discussions

This chapter discusses the results of the experiments performed in this study. It begins with the general discussion of properties of silicon material. Then, it is followed by the results of photoconductive and photovoltaic configuration; the two device configurations used in this study.

Silicon is an indirect material. Therefore, it has a slowly rising absorption coefficient. Fig. 5.1 (a) shows the absorption coefficient of silicon. The high absorption coefficient in UV region corresponds to shallow penetration depths. Fig. 5.1 (b) shows the light to current conversion in silicon, which peaks around 800 nm.

5.1 Electrical Measurements

5.1.1 Photoconductive Configuration

The principle of luminescent downshifting could not be demonstrated using the photoconductive configuration. The current-voltage measurement could not give any conclusive result, because of presence of high dark current. The high dark currents are involved due to the test done on low resistivity samples, with highest resistivity of 50 ohm-cm. The external quantum efficiency measurements were also not useful in this case.

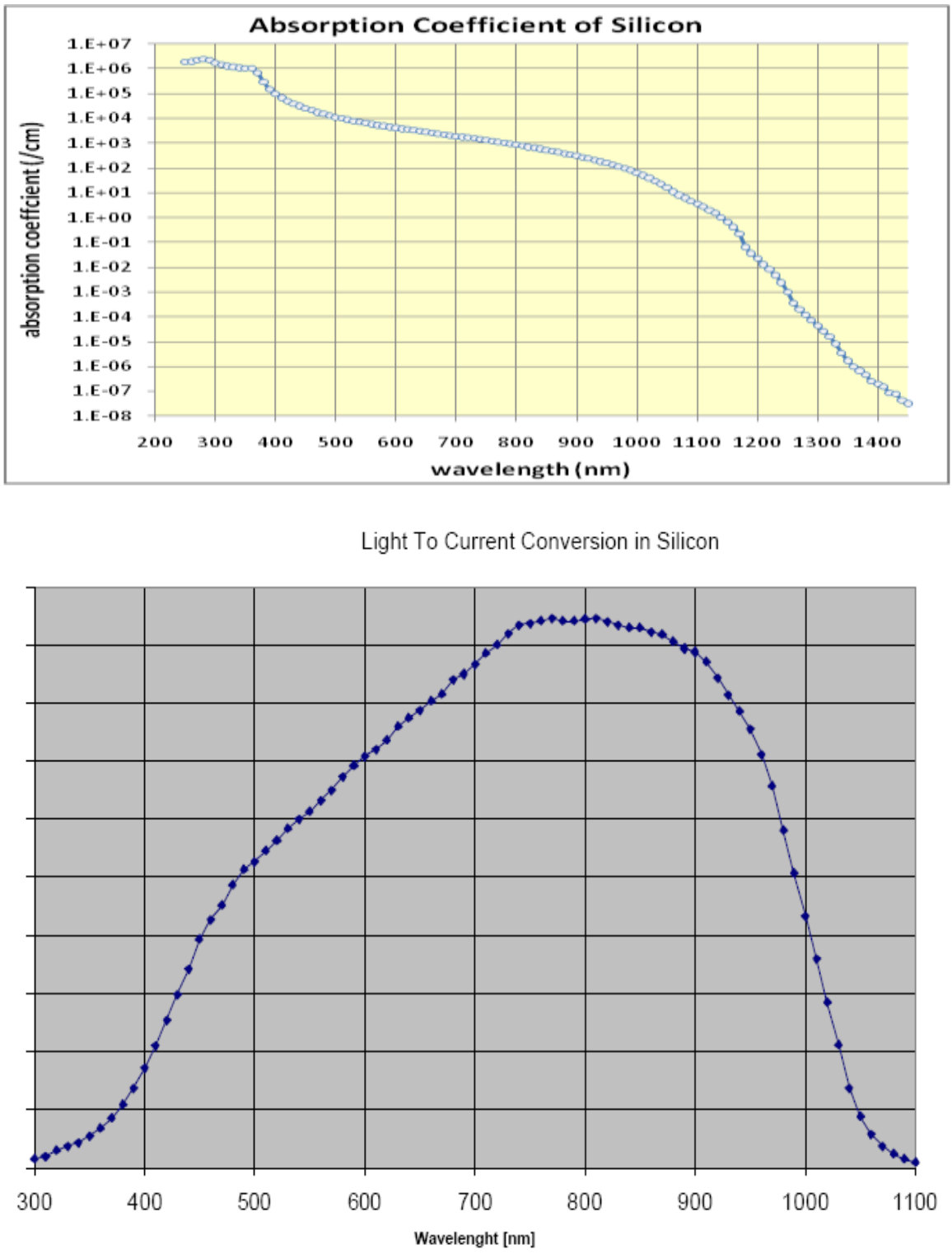

Fig. 5-1. (a) Absorption coefficient of silicon [34]. (b) Light to current conversion in silicon [35].

Initially, it was thought that quantum dots are emitting isotropically. But, the thin films of colloidal quantum dots are in between two different dielectric environments i.e. air and silicon. Therefore, the light gets effectively coupled into the higher refractive index material, which is silicon in this case. Hence, it is wrong to assume complete isotropic emission of quantum dots. The emission pattern of a fluorophore between two dielectric interfaces is considered in detail by Lukosz [36,37].

Still, there will be a tiny fraction of light which will be reflecting from the surface of silicon. Instead of using an anti-reflection coating, the contacts were deposited on back surface of silicon wafer. Close to ideal characteristics of ohmic contacts were achieved due to increased surface recombination velocity on the rough side of back surface. Fig. 5-2 shows the current-voltage characteristics of contacts deposited on the back side of wafer. Improvement in the current was visible in the current-voltage characteristics of the test structure with dots under UV light of 365 nm wavelength. Fig. 5-3 shows the current voltage characteristics of the test structure T21&T22 under dark and UV light. Highest increase of 30 % in current was observed at 1V. This validates that reduced reflection increases the photo generated current. Due to the presence of large number of surface states, the back side shows low surface current and poor response to the ultraviolet light. Fig. 5-4 shows the current comparison of the test structure on front and back surface of wafer. The significant improvement may be the result of extremely poor response of the back surface to the UV light.

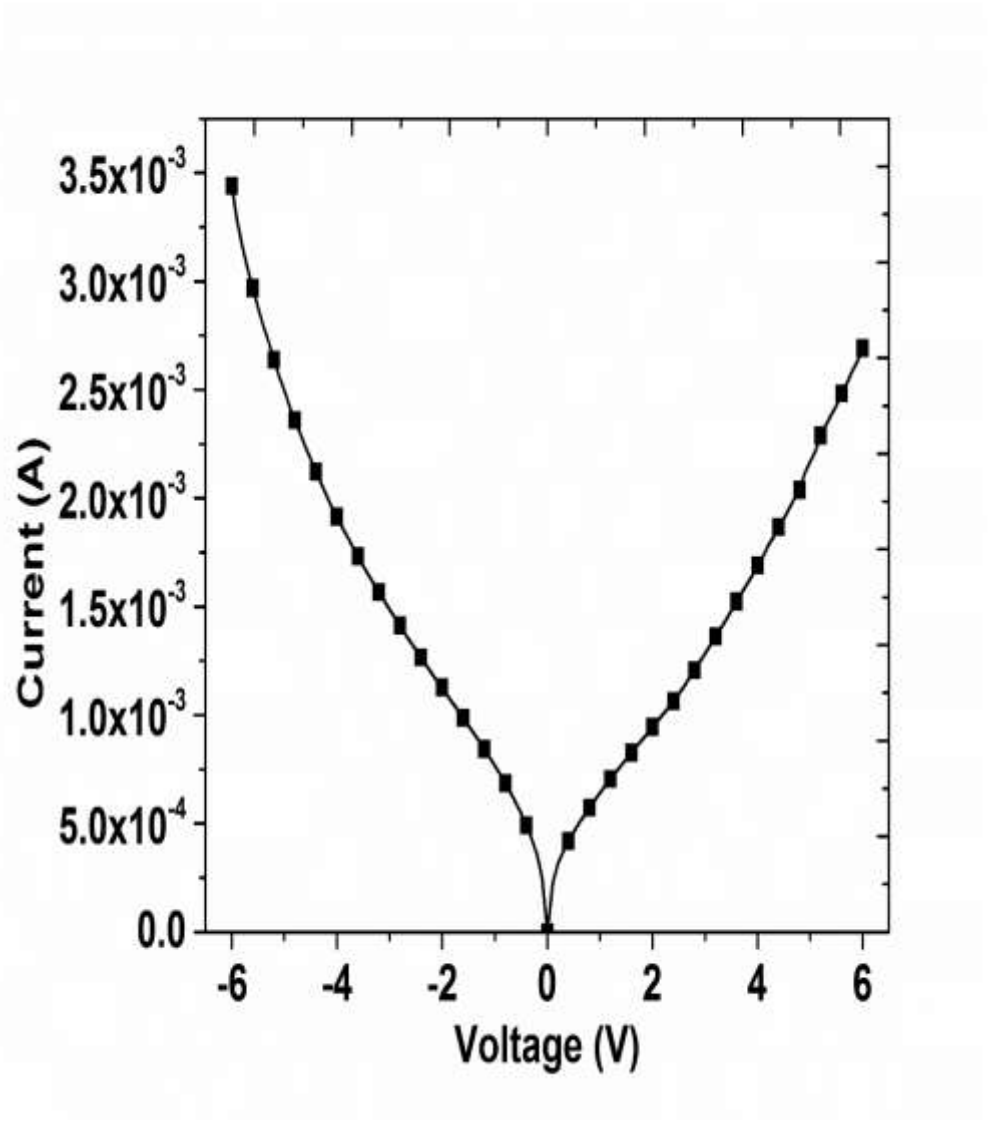

Fig. 5-2. Current-voltage characteristics of T21&T22 on back side of wafer.

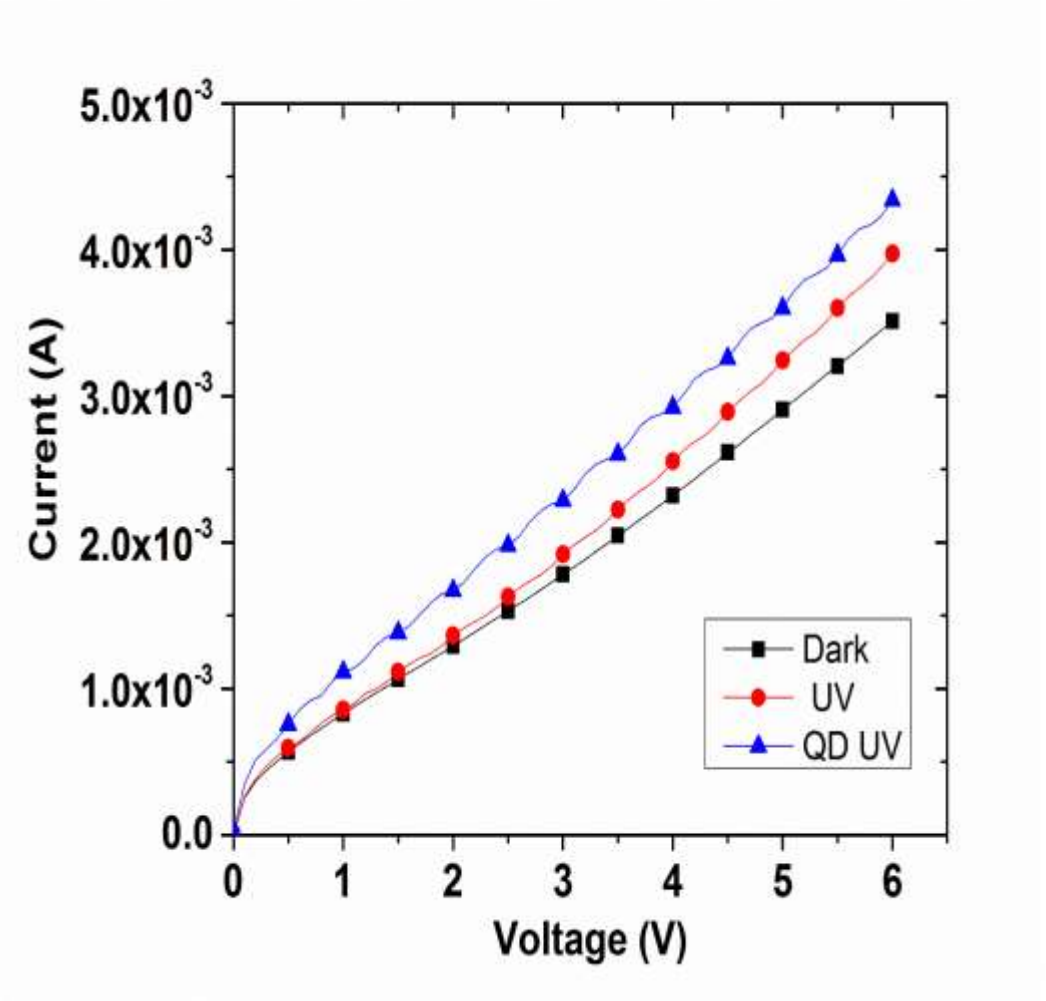

Fig. 5-3. Current-voltage characteristics of T21&T22 under dark and UV light.

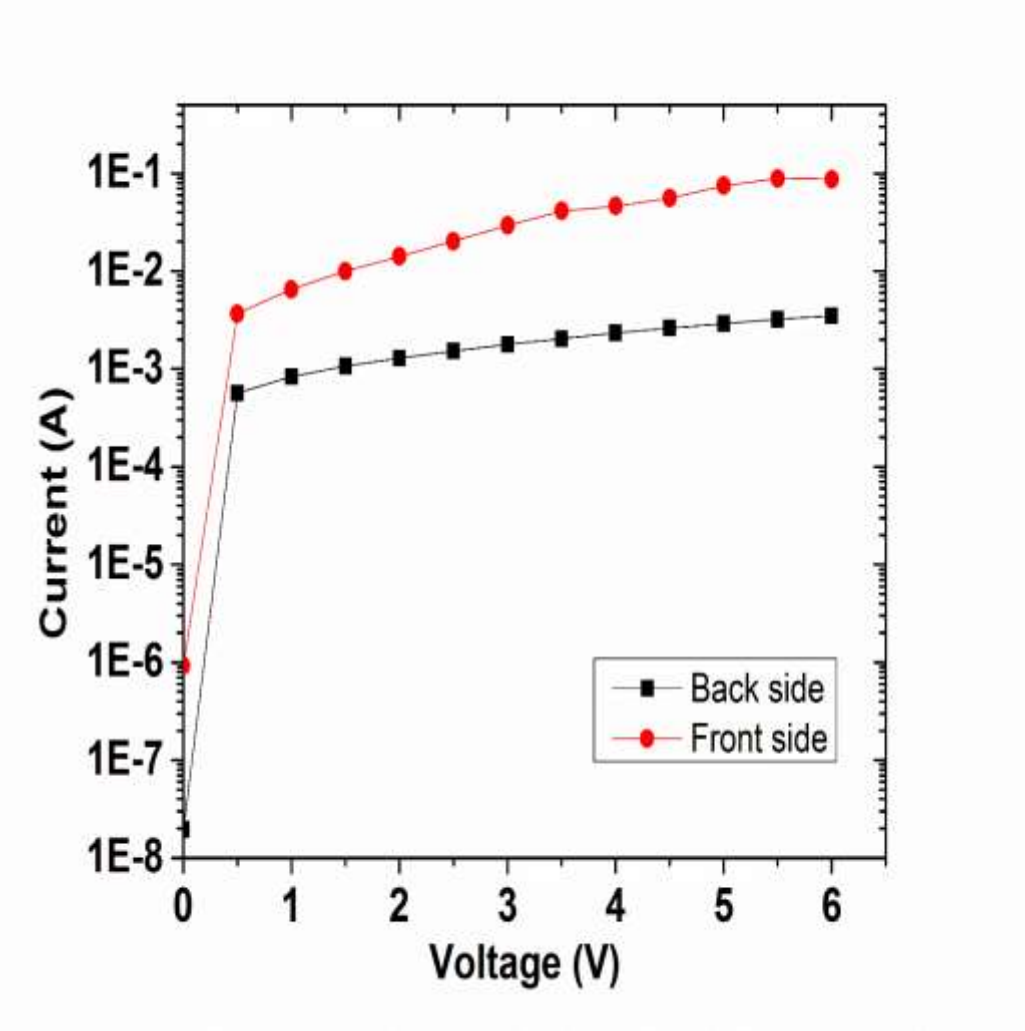

Fig. 5-4. Current-voltage comparison of front and back side of silicon wafer.

5.1.2 Photovoltaic Configuration

The fig. 5-5 shows the current-voltage characteristics of the photodiode on log and linear scale. The short circuit current (I_{SC}) improves by a factor of 6 after addition of QD's for an incident power of 29mW at 405 nm wavelength. This validates the increase in conversion efficiency, which is a result of the increased current generation. The open circuit voltage (V_{OC}) will not change significantly, as there is no change in the resistance of the device.

5.2 External Quantum Efficiency Measurements

The fig. 5-6 shows the external quantum efficiency curve, before and after deposition of QD's for different deposition thickness. The response of commercial silicon detectors is poor in near UV region, with external quantum efficiency of 15-30%, while it improves up to 27-35% for 40 nm thick QD layer.

The fig. 5-7 shows the average increase in external quantum efficiency with deposition thickness. The average external quantum efficiency is increased in near UV region by 9% for 10 nm deposition, 18% for 20 nm deposition, and 51% for 40 nm deposition of quantum dots.

(a)

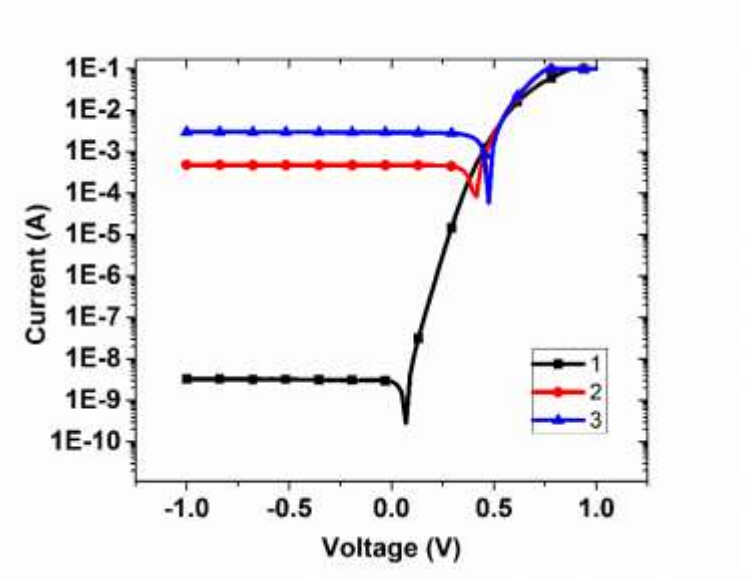

(b)

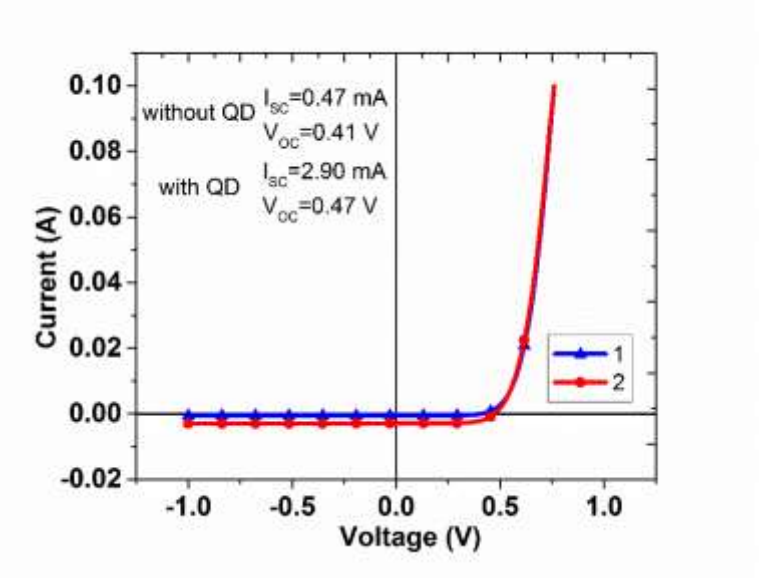

Fig. 5-5. (a) Plot of dark (1) and light (2,3) current-voltage characteristics of the photodiode at 405 nm before (2) and after 40 nm thick layer of QD (3) on log scale. (b) Same plot on linear scale showing current-voltage characteristics of photodiode before (1) and after 40 nm thick layer of QD (2).

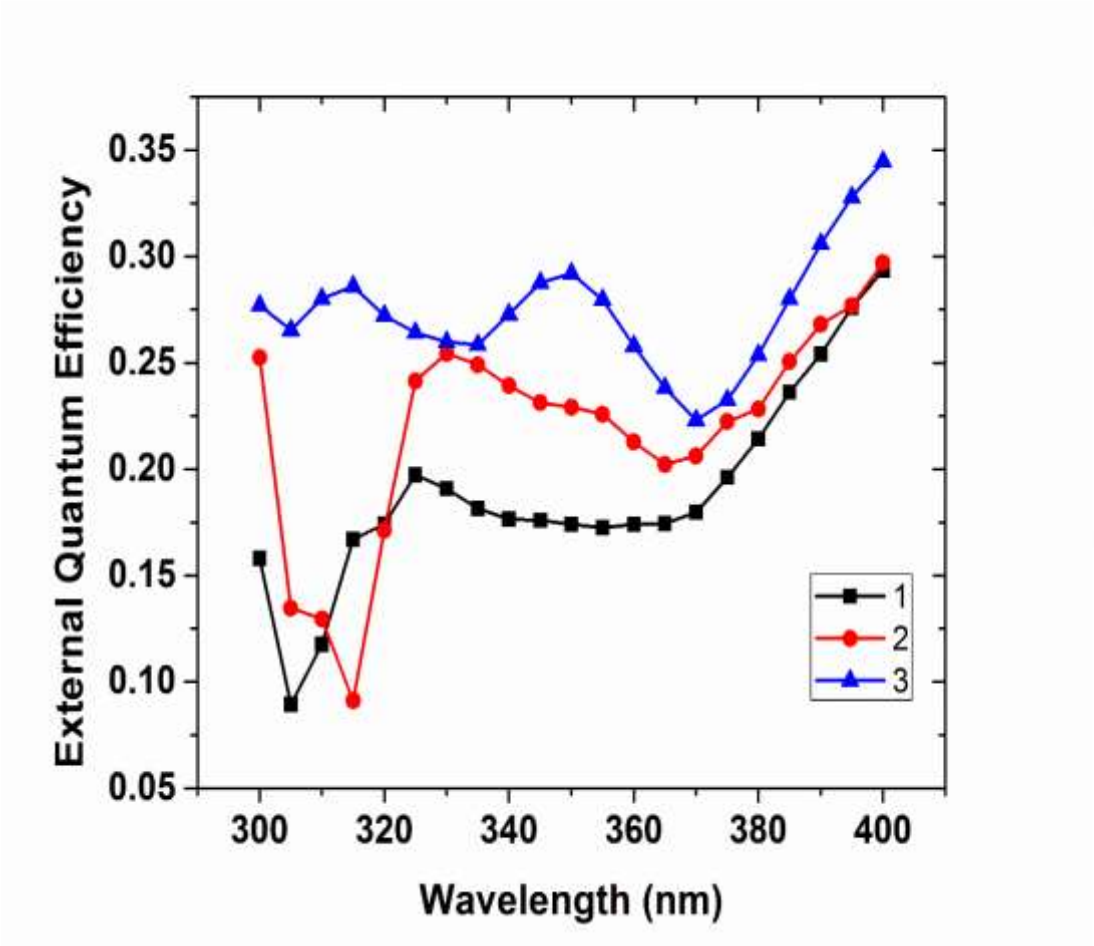

Fig. 5-6. EQE of silicon planar photodiode before (1) and after (2,3) CdSe/ZnS quantum dots- 20 nm deposition (2), 40 nm deposition (3).

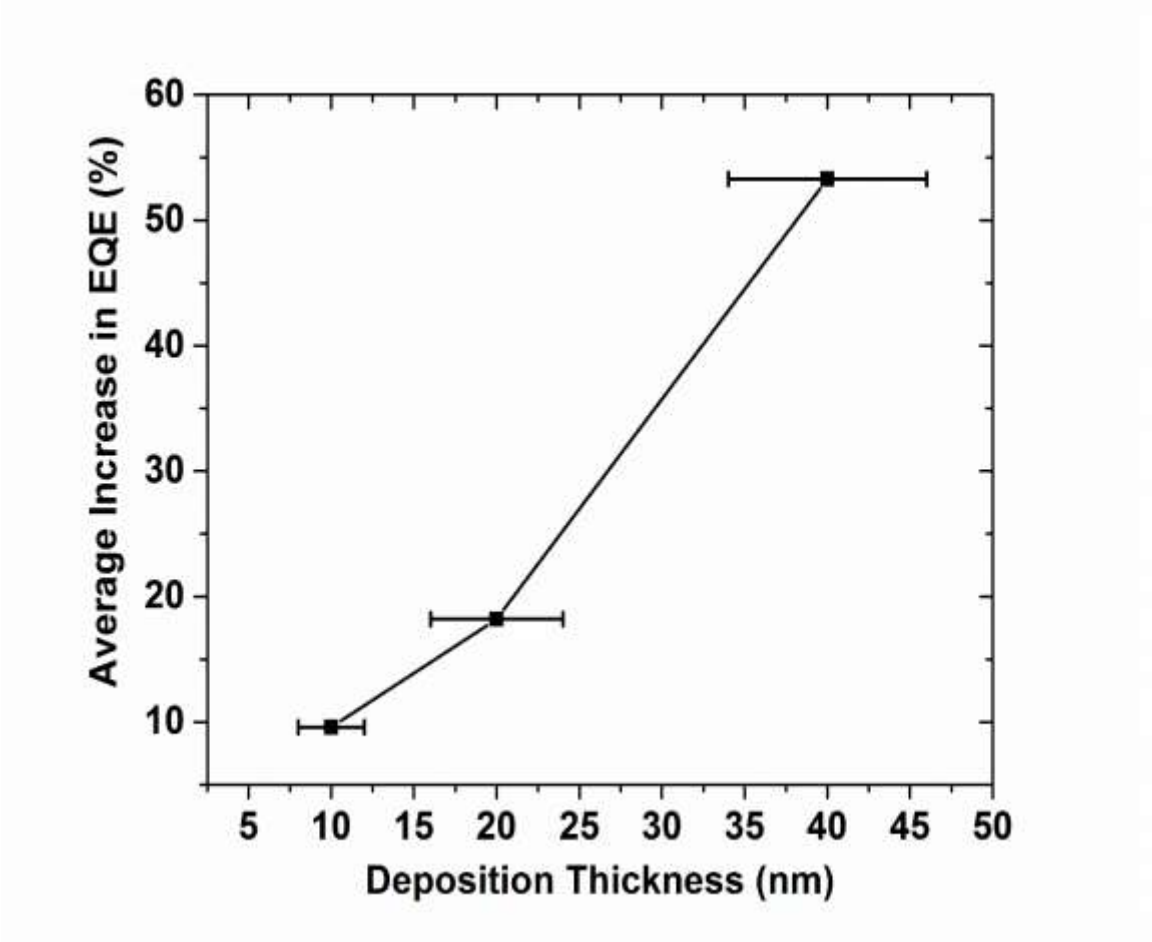

Fig. 5-7. Average increase in EQE with deposition thickness.

Chapter 6

Summary

In this thesis, principle of luminescent down-shifting has been demonstrated. It is utilized to improve the performance of the silicon photovoltaic detector in near UV region by sensitizing it with an ultra-thin layer of colloidal quantum dots. Thin film of 40 nm have increased the average external quantum efficiency in 300-400 nm by 51%. There is an improvement in short circuit current by a factor of 6 under laser excitation of 405 nm. The results demonstrate the effectiveness of quantum dots as luminescent down-shifting materials.

The mist deposition tool used in this study, provides us the ability to deposit films, as thin as few monolayers. It allows for the controlled deposition, and flexibility to deposit on circular as well as planar substrates. The optical density used in this study correspond to micro liters of quantum dot solution. Moreover, the solution left in the atomizer can be reused. Therefore, use of ultra-thin films and mist deposition makes the use of quantum dots cost-effective. Future work will involve finding of optimum thickness of CdSe/ZnS quantum dots, which will completely absorb the UV light.

The experimental results show that photovoltaic configuration is better than photoconductive configuration to show the downshifting phenomena. The presence of high dark currents in photoconductive configuration limited the analysis.

References

[1] L. Shi and S. Nihitianov (2012), "Comparative Study of Silicon–based UV Photo detectors," IEEE Sensors Journal, vol. 12 (7), p. 2453.

[2] E Monroy, F. Omnes, and F. Calle (2003), "Wide-band gap semiconductor ultraviolet detectors," Semiconductor Science Technology, vol. 18(4), p. 33.

[3] M. Razeghi and A. Rogalski (1996), "Semiconductor ultraviolet detectors," Journal of Applied Physics, vol. 79(10).

[4] S. Geyer, J. Scherer, N. Moloto, F. Jaworski, M. Bawendi (2011), "Efficient luminescent down-shifting detectors based on colloidal quantum dots for dual-band detection applications," ACS Nano, vol. 5(7), p. 5566.

[5] H.J. Hovel, R.T. Hodgson and JM Woodall (1979), "The effect of fluorescent wavelength shifting on solar cell spectral response," Sol. Energy Matter, vol. **2**(1), p. 19.

[6] R. Robinson, Z. Ninkov, D. Cormier, A. Raisanen, S. Bhaskaran, C. Beam, H. Ziegler, U. Arp and R. Vest (2013), "First Report on Quantum Dot coated CMOS CID arrays for the UV and VUV," Proc. Of SPIE Vol. 8859 88590 K-1.

[7] C. Cress, S. Hubbard, R. Robinson, R. Raffaelle, D. Wilt and S. Bailey (2007), "Radiation and thermal behavior of Quantum Dot Space Solar Cells," 20th Space Photovoltaics Research and Technology Conference: Ohio Aerospace Institute.

[8] http://www.sciencelearn.org.nz/Contexts/You-Me-and-UV/Science-Ideas-and-Concepts/Uses-for-UV, source Internet, Accessed on 4/1/2014

[9] X. Sheng, C. Yu, V. Malyarchuk, Y. Lee, S. Kim, T. Kim, L. Shen, C. Horng, J. Lutz, N. Giebink, J. Park and J. Rogers (2014), "Silicon-Based Visible-Blind Ultraviolet

Detection and Imaging Using Down-Shifting Luminophores," Adv. Optical Mater., vol. 2(4), p. 314

[9] Pallab Bhattacharya (1994), "Semiconductor Optoelectronic Devices," Prentice-Hall, Inc. New Jersey, p. 342.

[10] T. S. Moss, G. J. Burrel, and B. Ellis (1959), "Semiconductor Optoelectronics," Butterworths, London.

[11] M.J. Buckingham, and E.A. Faulkner (1974), "The theory of inherent noise in p-n junction diodes and bipolar transistors," The Radio and Elect. Eng., vol. 44, p.125

[12] R.J McIntyre (1966), "Multiplication Noise in Uniform Avalanche Diodes," IEEE Transactions on Electron Devices, ed. 13, p.164

[13] A. Rose (1955), "Space-Charge-Limited Currents in Solids," Phys. Rev., vol. 97(6), p. 1538.

[14] Giancarlo Barbarino, Riccardo de Asmundis, Gianfranca De Rosa, Carlos Maximiliano Mollo, Stefano Russo and Daniele Vivolo (2011), "Silicon Photo Multipliers Detectors Operating in Geiger Regime: an Unlimited Device for Future Applications, Photodiodes - World Activities in 2011", Prof. Jeong Woo Park (Ed.), ISBN: 978-953-307-530-3, InTech, DOI: 10.5772/21521. Available from: http://www.intechopen.com/books/photodiodes-world-activities-in-2011/silicon-photo-multipliers-detectors-operating-in-geiger-regime-an-unlimited-device-for-future-applic.

[15] E. Klampaftis, D. Ross, K. McIntosh and B. Richards (2009), "Enhancing the performance of solar cells via luminescent down-shifting of the incident spectrum: A review," Sol. Energy Matter Sol. Cells, vol. 93, p. 1182.

[16] W. Viehmann (1979), “Thin film scintillators for extended ultraviolet (UV) response silicon detectors,” Meas. Opt. Radiation, vol. 196, p. 90.

[17] G. Seybold and G. Wagenblast (1989), “New perylene and violanthrone dyestuffs for fluorescent collectors,” Dyes Pigments, vol. 11, p. 303.

[18] R.E. Sah and G. Baur (1980), “Influence of the solvent matrix on the overlapping of the absorption and emission bands of solute fluorescent dyes,” J. Applied Physics, vol. 23, p. 369.

[19] W.G.J.H.M.v.Sark, A. Meijernik, R.E.I. Schropp, J.A.M.v. Roosmalen and E.H. Lysen (2005), “Enhancing solar cell efficiency by using spectral converters,” Sol. Energy Matter Sol. Cells, vol. 87, p. 395.

[20] M. A. Reed (1993), "Quantum Dots," Scientific American, vol. 268, p. 118.

[21] Lukas Novotny and Bert Hecht (2006), “Principles of Nano-Optics,” University Press, Cambridge, p.310.

[22] C. Cheng and H. Yan (2009), "Bandgap of the core–shell CdSe/ZnS nanocrystal within the temperature range 300–373 K," *Physica E 41(5)*, p. 828.

[23] J. Szczech, J. Higgins and Song Jin (2011), “Enhancement of the thermoelectric properties in nanoscale and nanostructured materials,” J. Mater Chem., vol. 21, p. 4037.

[24] S. M. SZE and KWOK K. NG (2007), “Physics of semiconductor devices,” John Wiley & Sons, Inc., New Jersey, p.61.

[25] L.E. Brus, (1986), "Electronic Wave Functions in Semiconductor Clusters: Experiment and Theory," J. Phys. Chem. 90, p. 2555.

[26] A. Kshirsagar (2012), "Investigations into the formation of nanocrystalline quantum dot thin films by mist deposition process," Doctoral Dissertation, Penn State University.

[27] Tetyana Torchynska and Yuri Vorobiev (2011) 'Semiconductor II-VI Quantum Dots with Interface States and Their Biomedical Applications', Advanced Biomedical Engineering, Dr. Gaetano Gargiulo (Ed.), ISBN: 978-953-307-555-6, InTech, DOI: 10.5772/20628. Available from: http://www.intechopen.com/books/advanced-biomedical-engineering/semiconductor-ii-vi-quantum-dots-with-interface-states-and-their-biomedical-applications.

[28] http://www.lifetechnologies.com/us/en/home/references/molecular-probes-the-handbook/introduction-to-fluorescence-techniques.html, source internet, accessed on 4/2/2014.

[29] Y.Hu,Li Chen,K.Liu,J.Xiong (2012), "Fluorescence Properties of CdSe Quantum Dots Capped by ZnS" International Conference on Biological and Biomedical Sciences,Advances in Biomedical Engineering, vol. 9

[30] K. Shanmugasundaram (2008), "A study of the mist deposition and patterning of liquid precursor thin films," Doctoral Dissertation, Penn State University.

[31](http://curry.eas.gatech.edu/Courses/6140/ency/Chapter3/Ency_Atmos/Radiation_Solar.pdf), source internet, accessed on 3/2/2014.

[32] Klose, Jules Z., Bridges, J. Mervin, Ott, R. William (1987), "NBS Measurement Services: Radiometric Standards in the VUV" (http://www.nist.gov/calibrations/upload/sp250-3.pdf)(PDF), NBS Special publication (US Dept. of Commerce) (250-3)

[33] http://en.wikipedia.org/wiki/Ultraviolet, source internet, accessed on 3/5/2014.

[34] http://www.pveducation.org/pvcdrom/materials/optical-properties-of-silicon, source internet, accessed on 10/7/2013

[35] Spectral Response of Silicon Image Sensors, Arnaud Darmont, Aphesa (www.aphesa.com), White paper, April 2009

[36] W. Lukosz (1979), "Light emission by magnetic and electric dipoles close to a plane dielectric interface. III. Radiation patterns of dipoles with arbitrary orientation," J. Opt. Soc. Am., vol. 69(11), p. 1495

[37] W. Lukosz and R. E. Kunz (1977), "Light emission by magnetic and electric dipoles close to a plane interface. I. Total radiated power," J. Opt. Soc. Am., vol. 67(12), p.1607